



AUSTRIAN
MARSHALL PLAN FOUNDATION

Final report

“Investigating the role of variation in Bacteroides fragilis capsular polysaccharides in the pathogenesis of pouchitis”

By

Carolin Griewing

Bachelor programme

Medical and Pharmaceutical Biotechnology

External supervisors: Dr. Eugene B. Chang, M.D.
 Emma Liechty, DVM
 Daina Ringus PhD
Internal supervisor: Prof. (FH) Dr. Barbara Entler

Statutory Declaration

“I declare in lieu of an oath that I have written this bachelor paper myself and that I have not used any sources or resources other than stated for its preparation. I further declare that I have clearly indicated all direct and indirect quotations. This bachelor paper has not been submitted elsewhere for examination purposes.”

Datum: 24.02.2016



Carolin Griewing

Acknowledgements

First of all I would like show my gratitude to my supervisors, Emma Liechty DVM and Daina Ringus PhD, who greatly supported me during my internship and gave me the opportunity to be part of such an interesting project. I am really happy for their patience, motivation, enthusiasm and knowledge transfer I experienced throughout my internship. I appreciated the intense initial mentorship and the later takeover of individual projects.

I also want to thank the principal investigator Dr. Eugene B. Chang M.D., who made it possible for me to join the laboratory gaining experiences in many different fields and applications.

Moreover I want express my gratitude to Prof. Eva Werner and Prof. Harald Hundsberger for enormous effort and support throughout my study at the IMC University Krems.

I am especially thankful for the Austrian Marshall Plan Foundation and their financial support granted for my internship in the United States.

Last but not least my sincere gratitude is directed to Prof. Barbara Entler for her commitment and willingness to review my thesis and supporting me during my practical training semester.

Abstract

Inflammatory Bowel Diseases (IBDs), like Ulcerative Colitis (UC) and Crohn's Disease (CD), are chronic progressive immune disorders which appear in the gastrointestinal tract. The so called intestinal dysbiosis is the major trigger in the pathogenesis of IBD and is a result of the disruption of the host-microbe homeostasis.

I will focus on the clinical picture of pouchitis which is characterized as a nonspecific inflammation of the ileal pouch reservoir formed during the ileal pouch-anal anastomosis (IPAA) surgery. Through recent metagenomic analysis of pouch microbial communities, the microorganism *Bacteroides fragilis* has been found in abundance during episodes of pouch inflammation. A great significance is attached to capsular polysaccharide and its genetics. Three inflammation-associated genetic loci have been found within capsular polysaccharide-coding loci of *B. fragilis* pouch isolates. These potential virulence factors may contribute to enhanced host tissue destruction, tissue adherence and the ability to circumvent and evade the host immune response. *B. fragilis* therefore is capable of being a possible causative agent of pouchitis and other Inflammatory Bowel Diseases, IBDs.

In this thesis I address the hypothesis if there is evidence of altered interactions between the host and *Bacteroides fragilis* when capsular polysaccharide associated gene sequences are knocked out. Therefore I demonstrate a way to generate a mutant by knocking out one virulence associated gene, *peg.1727*, within the capsular polysaccharide-H (PSH) locus and methods to confirm its successful deletion in the chromosome of *Bacteroides fragilis*, followed by investigating the possible downstream effects of how the deleted gene sequence *peg.1727* influences the virulent characteristics of *Bacteroides fragilis*.

Table of Contents

Statutory Declaration.....	I
Acknowledgements	II
Abstract.....	III
Table of Contents.....	IV
List of Figures and Illustrations.....	VI
List of Abbreviations.....	VIII
1 Introduction	10
1.1 Inflammatory Bowel Diseases and related diseases	10
1.1.1 Outline of IBD diseases	10
1.1.2 Familial adenomatous polyposis.....	12
1.1.3 Pouchitis	12
1.2 <i>Bacteroides fragilis</i>	17
1.2.1 The cell envelope and its mode of action.....	17
1.2.2 The Virulence of <i>Bacteroides fragilis</i>	22
1.3 Principle of suicide vector mutagenesis.....	25
1.3.1 Suicide vector systems and counterselectable makers.....	25
1.3.2 Principle of double-cross-over recombination in targeted suicide vector mutagenesis.....	26
1.4 Thesis aim	27
2 Materials and Methods.....	28
2.1 Suicide vector mutagenesis.....	28
2.1.1 Fusion PCR.....	29
2.1.2 Plasmid purification.....	30
2.1.3 Digestion	30
2.1.4 Ligation	31
2.1.5 Transformation.....	31
2.1.6 Control PCR.....	32
2.1.7 Conjugation into <i>Bacteroides fragilis</i>	32
2.1.8 Passage and screening patch.....	33
2.2 Downstream suicide vector mutagenesis confirmation methods.....	33
2.2.1 DNA extraction and purification.....	33
2.2.2 RNA isolation	34
2.2.3 cDNA synthesis.....	34

2.2.4	PCR	34
2.2.5	Agarose gel electrophoresis.....	35
2.2.6	ExoSAP-IT PCR Cleanup	35
2.2.7	RT-qPCR	35
2.3	Competitive qPCR assay between peg.1727_psh mutant and P207	36
2.3.1	Growth curve and calculation for CFU/ml of peg.1727_psh mutant and p207	36
2.3.2	Competition assay	36
2.3.3	DNA extraction.....	37
2.3.4	qPCR Evaluation.....	38
2.4	Biofilm formation assay	38
2.5	Mandeval's capsule stain	39
3	Results	40
3.1	Suicide vector mutagenesis.....	40
3.1.1	PCR segments.....	40
3.1.2	Confirmatory Fusion PCR	41
3.1.3	Confirmatory transformation PCR	43
3.1.4	Confirmatory mutagenesis PCR of peg.1727 into B.fragilis P207	44
3.1.5	Confirmatory mutagenesis qPCR of downstream gene sequence peg.1740 expression.....	45
3.2	Transmission electron microscopy of peg.1727_psh and p207	46
3.3	Competitive qPCR assay between peg.1727_psh mutant and p207	47
3.3.1	Growth characteristics of peg.1727_psh and p207	47
3.3.2	Competitive qPCR assay	48
3.4	Biofilm formation assay	50
3.5	Mandeval's capsule stain	51
4	Discussion.....	53
4.1	Downstream suicide vector mutagenesis confirmation methods	53
4.2	Transmission electron microscopy of peg.1727_psh and p207	54
4.3	Competitive PCR assay between peg.1727_psh mutant and P207	55
4.4	Biofilm formation assay	56
4.5	Mandeval's capsule stain	57
5	Conclusion and future directions	58
	List of References	59

List of Figures and Illustrations

Figure 1: The triumvirate relationship of the three factors influencing the onset and pathogenesis of IBD.....	10
Figure 2. Anatomic illustration of the ileal pouch and its anastomosis	16
Figure 3: a graphic model of the gram negative cell envelope components of <i>B. fragilis</i>	19
Figure 4: genomic set up of the capsular polysaccharide biosynthesis loci	20
Figure 5: advanced genomic set up of the capsular polysaccharide biosynthesis loci	21
Figure 6: Illustration of the PSH, <i>peg.1727</i> locus.	24
Figure 7: Illustration of the PSA, <i>peg.2076</i> locus.	24
Figure 8: Principle of double-cross-over recombination	26
Figure 9: Illustration of the <i>p207</i> gene sequence	28
Figure 10: Gel electrophoresis confirming generation of segments 1 and 2 of <i>p207</i> <i>peg1727</i> gene for mutant construction.....	41
Figure 11: Gel electrophoresis confirming the fusion of segments 1 and 2 of <i>p207</i> <i>peg1727</i> gene for mutant construction.....	42
Figure 12: Gel electrophoresis confirming the insertion of the deletion construct <i>peg.1727</i> into plasmid <i>pKnock</i> in competent <i>E.coli</i> 217-1 cells.....	43
Figure 13: Gel electrophoresis confirming the insertion of the deletion construct <i>peg.1727</i> into <i>B.fragilis</i> <i>p207</i>	45
Figure 14: Graphic illustration of the expression of <i>peg 1740</i>	46
Figure 15: Transmission electron microscopy images of <i>p207</i> and <i>peg.1727_psh</i>	47
Figure 16: Graphic illustration of the growth characteristics between <i>B.fragilis</i> <i>p207</i> and <i>peg.1727_psh</i> in a logarithmic scale	48
Figure 17: Illustration of the growth of the competition cultures	49
Figure 18: Competition assay between <i>peg.1727</i> mutant and <i>p207</i> WT strain.	49
Figure 19: Biofilm formation of <i>B.fragilis</i> strains, <i>p207</i> , <i>p207Δ1727</i> , <i>p214</i> , 9343 after o/n anaerobic incubation at 37°C	50

Figure 20: Biofilm formation of *B.fragilis* strains, p207, p207 Δ 1727, p214, 9343 after 1h bile acid exposure of mid-log growth cultures.51

Figure 21: microscopic image of Mandeval stained p207 and peg.1727_psh under 100x magnification52

List of Abbreviations

IBD	Inflammatory bowel disease
UC	Ulcerative colitis
CD	Crohn's disease
IPAA	Ileal pouch-anal anastomosis
PS-X	Polysaccharide-X
GI	Gastrointestinal
FAP	Familial adenomatous polyposis
APC	Adenomatous polyposis coli
TNFα	Tumor necrosis factor α
IL-X	Interleukin-X
p-ANCA	Perinuclear anti-neutrophil cytoplasmic antibody
Bacteroides fragilis	B. fragilis
LPS	Lipopolysaccharide
OM	Outer membrane
TLR	Toll-like receptor
IM	Inner membrane
Pe	Periplasmic space
Pi	Pili
P	Porin
EP	Efflux pump
CPS	Capsular polysaccharide

IR	Inverted repeats
Mpi	Multiple promotor invertase
Ssr	Serine-specific recombinase
Tsrs	Tyrosine site-specific
RNAP	RNA polymerase
CPC	Capsular polysaccharide complex
PMN	Polymorphonuclear leukocytes
Ly-X	Lymphocyte
CSM	Counterselectable marker
SM	Selectable marker
WT	Wild type
Mut	Mutated
PCR	Polymerase chain reaction
Kan	Kanamycin
Amp	Ampicillin
BHIS	Brain Heart Infusion-supplemented
RT	Real time
CFU	Colony forming units
PBS	Phosphate buffered saline
OD	Optical density
CA	Sodium cholate hydrate
TCA	Taurocholic acid sodium salt
DCA	Sodium deoxycholate
EPS	Extracellular polymeric substance
TEM	Transmission electron microscopy

1 Introduction

1.1 Inflammatory Bowel Diseases and related diseases

1.1.1 Outline of IBD diseases

Inflammatory bowel diseases are chronic progressive immune disorders of the gastrointestinal tract. These three main components influencing the development of IBD, are the environment, gut microbiota and genetic susceptibility of the host.

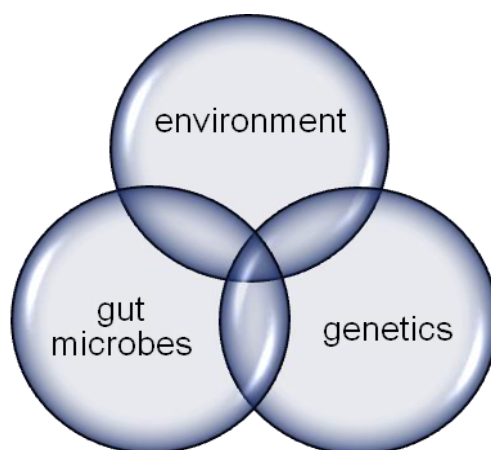


Figure 1: The triumvirate relationship of the three factors influencing the onset and pathogenesis of IBD.

An essential part of the pathogenesis of IBD is the disruption of the host-microbe homeostasis by an imbalance of structural and functional properties of the gut microbiota, so called intestinal dysbiosis. Two major clinical phenotypes of IBD have been investigated so far: Crohn's disease and ulcerative colitis (Dalal & Chang, 2014)

Ulcerative colitis primarily affects the colonic mucosa, whose immune response is found to be dysregulated. UC initially affects mucosa near the rectum and progresses up throughout the whole colon. UC is diagnosed at a higher frequency than CD and is most prevalent in northern European and North American countries characterized by a western, industrialized lifestyle. This insight implies that environmental factors such as diet or antigenic exposure play a major role in the pathogenesis

of UC. An elaborate health care system and western life style diet are environmental factors which may contribute to lower microbial exposure and associated infection rates in children. This may result in decreased development of the mucosal immune system. Furthermore, genetic susceptibility plays an important role. IBD occurs in 5.7% - 15.5% of first degree relatives. 47 susceptibility genes are so far known to contribute to the development of UC. These include genes involved in epithelial cell adhesion processes or leading to a dysregulated barrier function as a result of E-cadherin protein locus mutation. Gut microbes represent the third factor as they experience changes in the course of inflammatory gastrointestinal diseases. This leads to a loss of homeostasis between the microflora and mucosal immunity of the host. Together with environmental factors interaction in genetically susceptible hosts, it leads to the assumption to play a major role in the onset of UC (Dalal & Chang, 2014; Ordás, Eckmann, Talamini, Baumgart, & Sandborn, 2012).

The second clinical phenotype is Crohn's disease characterized as a relapsing chronic inflammatory disease appearing throughout the whole gastrointestinal tract beginning at the anus up to the mouth. Thereby it only affects mostly one specific part of the GI tract in one individual patient. The triumvirate interaction of environmental factors, dysregulated gut microbiota and CD susceptibility genes triggers the disease onset leading to an adaptive and innate perturbation of the affected host. Symptoms are fever, diarrhea associated with blood and mucus, abdominal pain and focal lesions in the gut wall developing into abscess and fistula formation over time. Similar to UC, there are 71 susceptibility genes of which 17 loci are shared with the UC repertoire. This gives rise to the fact that UC and CD are closely related on a genetic level. As with UC, environmental factors likely contribute to the development of CD. Factors of the western lifestyle like increased sanitation and hygiene standards, access to quality tap water, air pollution exposure, decreased amount of women breastfeeding and western lifestyle diet containing high amount of polyunsaturated fat and sugar, are hallmarks leading to a rising incidence of CD (Baumgart & Sandborn, 2012; Dalal & Chang, 2014). There is evidence that prior episodes of infectious gastroenteritis that alter the mucosal microflora is often correlated to the outbreak of CD. (García Rodríguez, Ruigómez, & Panés, 2006). The presence of

viral infections in already susceptible individuals has been observed to lead to increased susceptibility to CD. (Cadwell et al., 2010).

Over the last 50-100 years the incidence and prevalence of IBD has experienced a dramatic increase. This cannot be explained by genetic drift and is therefore seemed to be caused by altered environmental factors and a shift in societal norms by means of cultural westernization.

1.1.2 Familial adenomatous polyposis

Familial adenomatous polyposis (FAP) is an autosomal dominant disease resulting in colonic and rectal adenomas. Onset is typically in the second decade of life (Half, Bercovich, & Rozen, 2009; Plawski et al., 2013; Samadder, Gornick, Everett, Greenson, & Gruber, 2013). For the first years in the course of the disease, most patients do not experience any symptoms until the adenomas are growing to a certain extent in magnitude and multitude causing rectal bleeding, anemia and even cancer. On average, cancer development is seen 10 years after polyps appear and is associated with symptoms like abdominal pain, diarrhea and weight loss (Half et al., 2009). A autosomal dominant mutation on the adenomatous polyposis coli (APC) gene is the causative event for FAP development (Half et al., 2009; Samadder et al., 2013). The tumor suppressor gene APC is responsible for controlling the turnover of beta-catenin in the Wnt pathway (K. et al., 2011). Thereby it holds the function of a gatekeeper. In case of mutations in the APC gene adenoma development initiation and colorectal cancer progression are described. Physicians may recommend FAP patients undergo colectomy and ileal pouch anal anastomosis (IPAA) in order to prevent cancer. The IPAA surgery is explained in detail later in 1.1.3.5.

1.1.3 Pouchitis

1.1.3.1 General characteristics

Pouchitis is characterized as a nonspecific inflammation of the ileal pouch reservoir formed during the ileal pouch-anal anastomosis surgery. It is the most common

long-term complication of the ileal pouch surgery. Comparing the incidence of the outbreak of the inflammatory condition between different characterized patient groups, leads to the manifestation that around 23% to 46% of the patients having had the IPAA surgery will develop pouchitis. Patients with a UC background in the IPAA surgery (UC-IPAA) will have with a 50% probability a much in place higher likelihood to develop pouchitis compared to individuals suffering from FAP, where pouchitis is rarely observed (Shen & Lashner, 2008; Yu, Shao, & Shen, 2007)

1.1.3.2 Pathophysiology

The pathogenesis of pouchitis has not been investigated to its total extent, but there are hypotheses stating that in genetically susceptible hosts, luminal and mucosal bacteria communities are altered triggered by an abnormal immune response of the host. As a result of the surgery in which the anatomy of the bowel is changed, an environment prone to inflammation may be created. Within the newly created pouch, distal ileal function shifts from nutrient absorption to an artificially created storage reservoir with a mucosa that is exposed to feces. These changes qualitatively and quantitatively may be driving factors in the outbreak of pouchitis (Shen & Lashner, 2008). Regarding host responses there are overlaps in the cytokine expression between UC and pouchitis. Nevertheless pouchitis is more than just a revision of the UC disease process. An increase of activated T-cells has been shown to be accompanied by elevated marker expression, like CD25, CD30 and CD27. Followed by T-cell and several other immune cell activation, cytokine expression gets upregulated, too (Yu et al., 2007). Profiles of abnormal cytokines have been shown in the pathogenesis of pouchitis along with a deregulated immunoregulatory and proinflammatory cytokine production (Goldberg et al., 1996). For example, TNF α is a proinflammatory cytokine found in high numbers in inflamed mucosa released by monocytes and macrophages. This event of TNF α secretion is seen as a second mechanism in the pathogenicity of pouchitis (Goldberg et al., 1996). Similar to UC there are also other inflammatory mediators whose production is increased. Into this category fall other cytokines like IL-1 β , IL-6 and IL-8, platelet-activating factor, cell adhesion molecules like E selectin, proinflammatory neuropeptides, matrix metalloproteinase -1, -2, -9, -14, macrophage inflammatory protein 2 α and inducible nitric oxide. Besides

them also an abnormal production in immunoregulatory cytokines like IL-2, IL-4, IL-10 and interferon- γ are observed. Between these two major mediators exists an imbalance in pouchitis patients (Shen & Lashner, 2008; Yu et al., 2007).

It has been observed that pouchitis occurs to a greater extent in patients with previous UC and there is evidence of similar characteristics regarding abnormal immune responses and the clinical phenotype between UC and pouchitis. Taking these observations into account a part of pouchitis might be considered as a relapsing UC-like disease in the ileal pouch. This suggestion is underlined by supporting factors such as that the pouch mucosa is exposed to fecal stream, no movement in the pouch itself and an elevated microbial amount, which themselves give rise to the explanation of a change in the ileal pouch mucosa leading to a mimicry of colon like epithelia in UC.

1.1.3.3 Risk factors and clinical presentation

There have been several risk factors for pouchitis reported which vary depending on the type of pouchitis. Disease characteristics can range from chronic, antibiotic-refractory to acute, antibiotic-responsive depending on the individual patient. Besides genetic alterations in NOD2/CARD15 and IL-1 receptor antagonist there are more risk factors for pouchitis. These include increased backwash ileitis, a TNF allele 2 in a non-carrier status, serum perinuclear anti-neutrophil cytoplasmic antibodies (p-ANCA), pre-proctocolectomy thrombocytosis, consuming non-steroidal anti-inflammatory drugs and non-smoking (Bonizzi et al., 2004; Shen & Lashner, 2008; Yu et al., 2007)(Angriman, 2014; Shen & Lashner, 2008; Yu et al., 2007).

Pouchitis is characterized by clinical manifestations such as urgency, elevated stool frequency, abdominal cramps, incontinence, tenesmus and pelvic discomfort. In advanced disease, symptoms like dehydration, fever and malnutrition can appear (Shen & Lashner, 2008; Yu et al., 2007).

1.1.3.4 Relationship between pouchitis and the pouch microbiota

The interaction of intestinal microbiota associated to the mucosa and the pathogenesis of inflammatory diseases in the gastrointestinal tract have been extensively investigated. The shift from a balanced microbiota contributing to anti-inflammatory and immunomodulatory effects to a deregulated unbalanced microbial composition leads to a possible toxin driven mucosa damage or abnormal immune responses (Angriman, 2014; Tamboli, Neut, Desreumaux, & Colombel, 2004).

Studies demonstrated that there is a compositional change in microbiota when comparing UC-IPAA to FAP-IPAA patients. UC-IPAA patients showed higher amounts of *Proteobacteria* and lower levels of *Bacteroidetes* as well as a smaller bacterial diversity compared to the FAP-IPAA patients (McLaughlin et al., 2010; Zella et al., 2011). These observations lead to the hypothesis that the unbalanced microbiota puts UC patients to risk by either diminishing the microbial diversity or elevating the possibility to stimulate the immune system, which both would lead to an inflammation of the mucosa (Angriman, 2014). Summarizing different studies there is evidence that the microbial dysbiosis in the pouch of UC-IPAA patients plays a major role in the pathogenesis of pouchitis, but may not be the only reason triggering the inflammation. It should be more seen as factor for the predisposition of pouchitis in genetically susceptible patients. Further factors such as overexpressed defensins or altered epithelial membrane functions could lead to worsening in dysbiosis and onset of chronic immune response of the mucosa (Angriman, 2014).

1.1.3.5 Ileal pouch anal anastomosis surgery

The ileal pouch anal anastomosis surgery has been become more and more popular throughout the last fifteen years. The treatment is used in patients with intractable UC and FAP by removing the affected large bowel and establishing a new ileal pouch reservoir, which is connected to the rectum. Over the past years the procedure was improved by figuring out which configuration, S, J, H, W, of the pouch is the best option to take. After several investigations the J pouch configuration was

chosen to be the standard technique to use since its evacuation efficiency and easier establishment (Kircher, Koruda, Mark J., & Behrns, Kevin E., 2003; McGuire, Brannigan, & O'Connell, 2007).

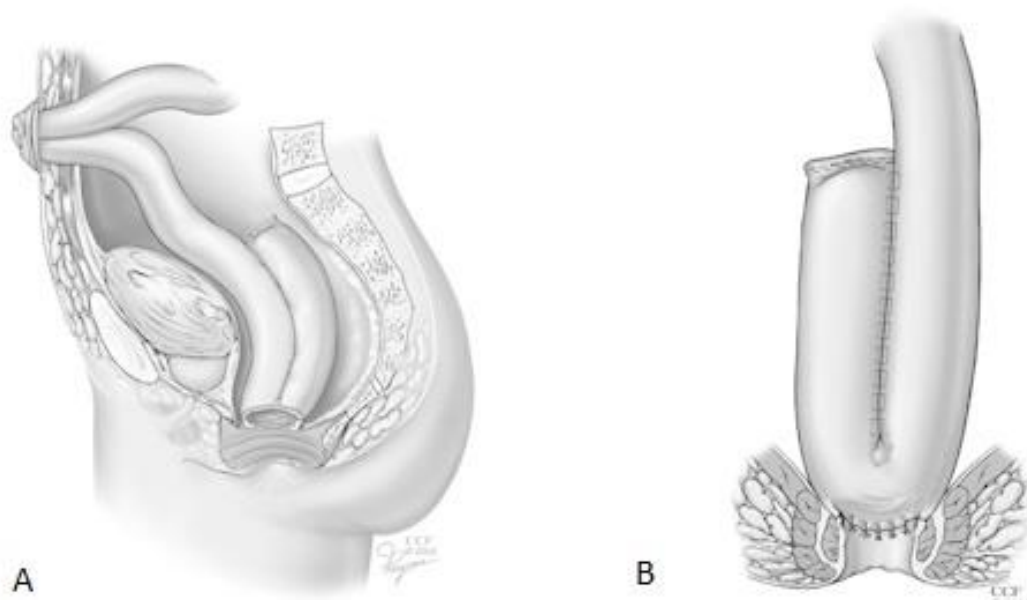


Figure 2. (A) Ileal pouch anal anastomosis (B) J-pouch anastomosed to anal canal (Martin & Vogel, 2013)

The operation takes the terminal small intestine, sews the end into a J shape and then attaches the artificial pouch to the anal sphincter muscle (see figure 1.B). The result is an artificial reservoir for stool being able to conduct bowel movements both in a controlled or predictable fashion (Kircher et al., 2003). Surgeons anastomose the J-pouch to the top of the anal canal preserving the mucosa in the anal transitional zone. This reduces the likelihood of incontinence, anal sphincter damage and the development of mucosal diseases (McGuire et al., 2007). Beneficial effects of the surgery are eradicating associated symptoms like urgency and diarrhea, reducing the frequency of medication intake, no necessity of attending colonoscopies or flex sigmoidoscopies and overall improving the patients' quality of life (Kircher et al., 2003). After extensive investigations IPAA was chosen to be the safest, long term procedure in treating UC and FAP implicating increased quality of life compared to patients' undergone permanent ileostomy. As pointed out previously IPAA still stays a challenge as a subset of UC patients develop pouchitis after surgery, which actuators are not yet investigated in a great extent (McGuire et al., 2007).

1.2 *Bacteroides fragilis*

The human body mainly consists of bacterial cells which are found to be with 90% the major group of residents in humans. In the human the largest concentration of microbial organisms are found in the gastrointestinal tract, the core community of which varies from person to person (Wexler, 2007). In adults, *Firmicutes* and *Bacteroidetes* are found more frequently than phylotypes like *Proteobacteria* and *Actinobacteria* (Lozupone, Stombaugh, Gordon, Jansson, & Knight, 2012).

Among *Bacteroidetes*, the strain *Bacteroides_fragilis* (*B. fragilis*) makes up only 1-2% of the total mammalian gastrointestinal microflora. Nevertheless it is detected as the most abundant strain in human intestinal infections, inflammation, bacteraemia and sepsis (Pumbwe, Skilbeck, & Wexler, 2006). *B. fragilis* is characterized as an anaerobic, partly aero-tolerant, gram negative, ubiquitous gut commensal which is, based on its properties, mainly found in the gastrointestinal tract (Huang, Lee, & Mazmanian, 2011). One crucial property is the existence of two different behavioural forms, in which *B. fragilis* is found. On one side the microbe can provide a beneficial relationship between the host and itself, acting as a commensal. Polysaccharide (PS) metabolism, the ability to trigger immune responses based on the specific polysaccharide production and bile tolerance are characteristics based on the commensal behavioural form. On the other side *B. fragilis* shows a controversial pathogenic property characterized by circumventing antimicrobial treatment or host immune responses, destroying the host tissue or secreting factors needed for the adherence to human infectious tissue. The reason for these divergent properties is the composition and regulation of the cell envelope of *B. fragilis* (Pumbwe et al., 2006).

1.2.1 The cell envelope and its mode of action

B. fragilis makes up a high percentage with small variation in their abundancy in the gastrointestinal tract of human beings. Throughout its evolutionary development *B. fragilis* has generated certain strategies which enable the microorganism to compete in the gut environment. These include the metabolism of nutrients, attachment and the ability to bypass signals, which are either send from the exterior or from the host

itself. The structural composition of the *B. fragilis* cell envelope is the major reason why the microorganism is found in both commensal and pathogenic acting state. This special characteristic gives rise to its ability to invade, defend and trigger pathogenicity (Pumbwe et al., 2006).

1.2.1.1 General cell envelope structure

For further investigations on the complexity of the controversial character and response of *B. fragilis*, we have to take a closer look at the overall cell envelope structure. As depicted in Figure 3 the cell envelope is a complex structure made up of a protruding layer arrangement on which certain surface molecules bind. This structure is essential for the existence of *B. fragilis* in the mucosal layer of the intestinal crypts and gives rise to its ability to form abscesses. Pili, fimbriae and adhesins are the three major surface structures, which primarily are used in the course of attachment to intestinal cells and mucus. Besides them also the host provides factors like lectin-like adhesins, which promote the binding of *B. fragilis*. They serve as one of the most abundant receptors in the attachment process (Pumbwe et al., 2006). There is evidence that also other receptors like sialic acid and different sugars are displaying structures like adhesin receptors and are thereby involved in promoting adhesion (Domingues et al., 1992). The lipopolysaccharides (LPS) which are displayed on the cell envelope's outer membrane (OM) hold two main functions. While they contribute as a protective mechanism for the lipid part buried in the OM, the LPS also serve as an adhesion factor. The latter is however only weakly recognized by the toll-like receptor 4 (TLR4) (Pumbwe et al., 2006)

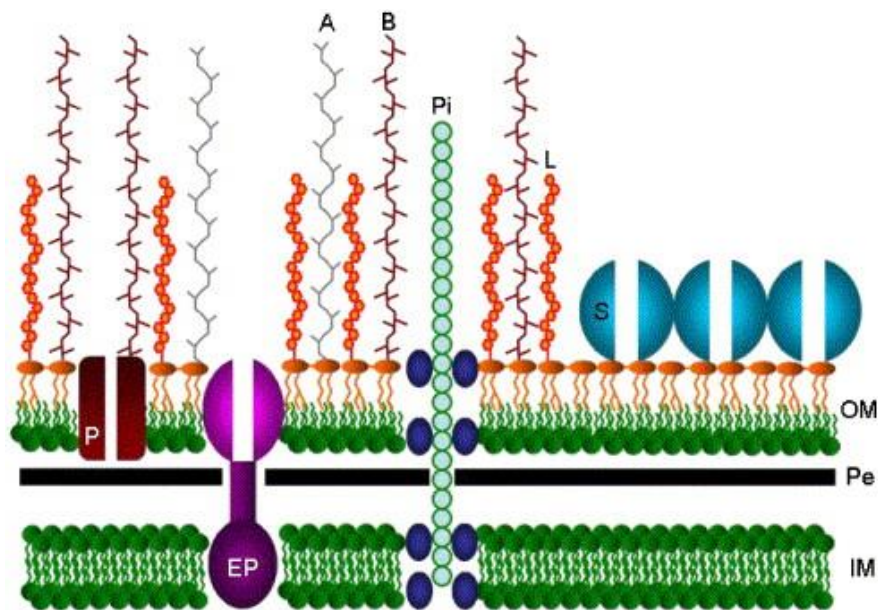


Figure 3: a graphic model of the gram negative cell envelope components of *B. fragilis*. It is made up of 3 major parts in a protruding manner, namely the inner membrane (IM), the outer membrane (OM) and the periplasmic space (Pe), which are interrupted by certain proteins. Pili (Pi) with attached export proteins (blue) are spread out over the whole cell envelope. For supplying the cell with the mechanism of molecule diffusion through the cell envelope, an outer membrane protein porin (P) is integrated into the OM. In order to be able to export toxins such as antibiotics, heavy metal ions or other toxins, there are efflux pumps (EP) installed which direct these toxins out. A characteristic feature of the cell envelope are the surface molecules attached on the OM. Lipopolysaccharides are depicted in orange. Depending on a rough or smooth characterized surface, side chains (L) are attached or not. Concerning *B. fragilis* there are two main capsular polysaccharides namely polysaccharide A (A) and B (B). Together with the LPS side chains and distinct other surface polysaccharides they built up the glycocalyx. The shown S layer (S) is not observed in *B. fragilis*, but still found in other *Bacteroides* species (Pumbwe et al., 2006).

1.2.1.2 Capsular polysaccharides and its regulation via DNA inversions

The ability of *B. fragilis* to present different surface structures which vary in their capsular polysaccharides arrangements gave rise to develop an adaptive advantage in the ecological colon environment allowing the microorganism to dominate in the gastrointestinal tract. Features are implementing colonization, reciprocal host pathogen and symbiont interactions (Krinis et al., 2001; Liu et al., 2008).

With providing both pro-inflammatory and immunoregulatory characteristics polysaccharide A (PSA) is the most predominantly expressed CPS (Surana & Kasper, 2012). The expression of the cell surface structure and overall net charge is very distinct between PSA and PSB. PSA is made up of repeating tetrasaccharide units

and displays a net charge balance of positive charged amino groups and negative charged carboxyl groups. On the other side PSB is built up of hexasaccharides units in a repeating manner and holds an unbalanced net charge of one positive amino group and two negative charged groups namely one galacturonic acid residue and one phosphonate group. This unique charge motif which differs from PS to PS and shows both charges on their capsular surface, makes the *B. fragilis*'s CPC very unique compared to other bacterial polysaccharides (Pumbwe et al., 2006).

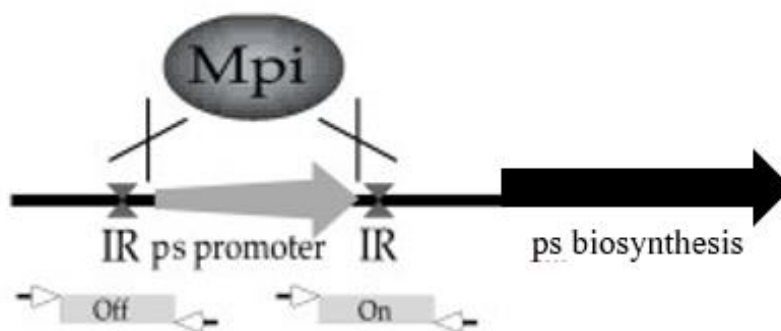


Figure 4: genomic set up of the capsular polysaccharide (CPS) biosynthesis loci illustrating the inverted repeats (IRs) flanking the polysaccharide biosynthesis promoter. The enzyme called Multiple promotor invertase (Mpi) acts on the IR regions and promotes recombination. As a consequence the promoter is either turned "on" or "off" which is relevant for the downstream polysaccharide biosynthesis (Liu et al., 2008)

Currently there is evidence that there are eight distinct capsular polysaccharides (CPS) biosynthesis loci in the genome of *B. fragilis* called polysaccharide A – polysaccharide H (PSA – PSH). These loci are found in an operon structure comprising 11-22 genes and present a commonly organized genetic structure (see Figure 4) (Chatzidaki-Livanis et al., 2010; Krinos et al., 2001; Liu et al., 2008). Displaying this multiplicity of CPS loci is a unique characteristic associated to *B. fragilis* (Krinos et al., 2001). Seven out of the eight CPS loci have a promoter ranging from 19 to 25 bp in length and depending on the orientation of the inverted repeats (IRs), the promoter is switched "on" or "off". These IRs are placed next to the promoter region and by changing the promoter state from "on" to "off" or vice versa, the transcription of the downstream genes are regulated. The enzyme multiple promotor invertase (Mpi) is the actuator catalyzing the inversion of the IRs. Mpi belongs to the serine-specific recombinase (Ssr) family. Beside the Ssr family also the tyrosine site-spe-

cific (Tsrs) recombinases exists, which both are grouped to be DNA invertases. Regarding their action, Tsrs family DNA invertases are important actors in fimbriae phase variation, while DNA invertases of the Srs family are regulators of a certain site being incorporated by phages into bacteria (Coyne et al., 2003).

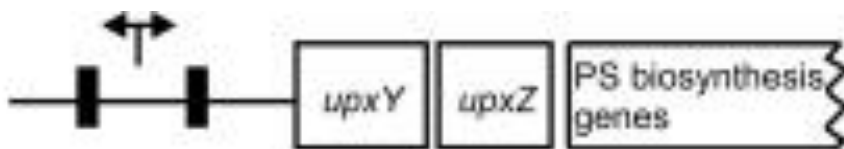


Figure 5: advanced genomic set up of the capsular polysaccharide biosynthesis loci displaying the IRs (black boxes), downstream UpxY and UpxZ genes coding for transcriptional antitermination factors and terminal PS biosynthesis genes. The possibility of inverting promoters is depicted by the arrows pointing in two different directions (Chatzidaki-Livanis, Coyne, & Comstock, 2009).

Having a look on Figure 5 there are additional genes found in each of the eight loci, which are located downstream of the second IR sequence. 126 to 224 bp untranslated DNA is found between the second IR sequence and the first gene coding for proteins of the UpxY family depicting transcriptional antitermination factors. Depending on the specific polysaccharide the sequence belongs to, the letter x can be exchanged by the corresponding letter a-h. The proteins which are encoded by the gene sequence are found to be highly similar ranging from 38 to 78 %. The UpxY proteins regulate and control the transcription of the PS synthesis. Thereby mainly the NusG motif is involved, which interacts with the RNA polymerase (RNAP) (Chatzidaki-Livanis et al., 2009; Krinos et al., 2001). Thereby transcriptional termination is prevented. This brings along an extended rate of transcription and the possibility to transcribe long sequences (Chatzidaki-Livanis et al., 2009). Directly after the UpxY gene there is a second gene termed UpxZ located with a similar correspondence of 44% to 72% between the eight different loci. The UpxZ family proteins are not involved in regulating their specific PS, they bypass the synthesis of heterologous PS group. The PS biosynthesis genes follow these two Upx genes, which are of high significance as they code for specific enzymes catalyzing the PS synthesis (Chatzidaki-Livanis et al., 2010).

1.2.2 The Virulence of *Bacteroides fragilis*

In the course of investigating the virulence of *B. fragilis*, three main bacterial characteristics have been shown to have a significant impact. These virulence factors cover tissue destruction, tissue adherence and the ability to circumvent and evade the host immune response. *B. fragilis* holds certain adhesion molecules like fimbriae and agglutinins, which act as adhesins and support them thereby in the interaction process with the host tissue. Phenotypic properties which enable *B. fragilis* to evade the host immune response includes its unique polysaccharide capsule composition, certain enzymes and lipopolysaccharides. Enzymes found to play an important role in the virulence of the microorganism are proteases, hemolysins, neuraminidases and histolytic enzymes. Histolysis is the disintegration of organic tissue. *B. fragilis* therefore is capable of destroying the host tissue making the mammalian body prone to infection (Wexler, 2007).

1.2.2.1 Role of the bacterial capsule and T-cells on the immune system

A paper published by Kasper and colleagues (Kasper & Seiler, 1975) states that the bacterial capsule is one of the major virulence factors in *B. fragilis* by being an important factor in inducing abscess formation. His group showed that bacteria of this species lacking the capsule were not able to induce abscesses in a rat model, while encapsulated strains, whose bacterial cells have been heat killed before, did show a high capability of forming abscesses. In addition they illustrated that the capsular polysaccharide complex (CPC), serving as a protective shield for *B. fragilis* against the immune system recognition, is the main structure within the bacterial cell serving as the active source of inducing abscesses in the host (Tzianabos, Kasper, & Onderdonk, 1995). This unique and distinct property of the CPC enables *B. fragilis* to play the major role in forming abscesses, even without the need of a second synergistic organism (Shapiro et al., 1986).

As identified out in 1.2.1. the capsular surface containing the unique charge motif exposing both negative and positive charges, makes the CPC of *B. fragilis* unique from other bacterial polysaccharides. Tzianaos, Kasper and Onderdonk showed the evidence of a diverging character between PSA and PSB regarding their ability to

actively promote abscess formation (Tzianabos et al., 1995). In their study they investigated in a test rat the needed amount of the individual polymer in order to create a 50% abscess formation (AD_{50}). They detected that PSA needed a lower dose (AD_{50} of 0.67 μ g) in order to achieve the aim compared to PSB (AD_{50} of 25 μ g) and CPC (AD_{50} of 22 μ g) which required a higher amount to reach the same point. Furthermore they indicated the necessity of the balanced charge character of PSA for the abscess formation promoting potential since chemically modified PSA altering its charge balance, decreased the PSA inductive potential in a 2 fold manner. There is still no approved evidence on how the host immune system is effected by the charge motif of the CPC. Nevertheless theories exist suggesting that the reactive properties of the attached and exposed groups on the oligosaccharide of PSA and PSB are of importance. One theory takes a Schiff base reaction into consideration. A Schiff base is a chemical structure formed between an aldehyde and a primary amine. This reaction involves the interaction between a free amino group of the PSs and the carbonyl group presented on T-cells and is stated to have a possible effect on driving the immune response promotion in inducing abscess formation in the host (Tzianabos et al., 1995).

Beside the role of CPC in inducing abscess formation, there is evidence that T-cell are a driving factor in its regulation when exposed to *B. fragilis*. The method of abscess formation constitutes the major difference between the majority of bacterial PS and the unique CPC of *B. fragilis*. While most bacterial PS provoke hormone responses in a T-cell-independent way, the CPC is shown to be working in a T-cell-dependent manner (Tzianabos, Onderdonk, Rosner, Cisneros, & Kasper, 1993). In the course of a *B. fragilis* exposure and abscess induction, an establishment of precursor or helper T-cells is observed. During the formation of abscesses an aggregation of polymorphonuclear leukocytes (PMN) cells is observed, which is suspected to play an important role in initiating immune host responses next to T-cells. Phenotypically these T-cells are known to be either inducer or precursor T-cells and possess a combination of lymphocyte 1 and 2 (Ly-1, Ly-2) surface markers. Until now there is no clear evidence on how these precursor T-cells collaborate with the PMN cells, which are localized in the abscess tissue. Some theories suggest that

after bacterial exposure there is a migration of lymphocytes into the peritoneum triggering PMN Ly-1 and Ly-2 entry. This suggested mechanism is said to start the abscess formation process (Shapiro et al., 1986; Tzianabos et al., 1995)

1.2.2.2 Capsular polysaccharides associated virulence genes

As discussed in 1.2.2.1. the capsular polysaccharides of *B. fragilis* are known to be one of the major virulence factors in the pathogenesis of IBD (Kasper & Seiler, 1975). Recently our group has identified three virulence associated genes, which are abundant in inflamed pouches. These virulence associated genes, namely WcbM, NeuB and CpsM, are found on certain capsular polysaccharides and facilitate different functions.

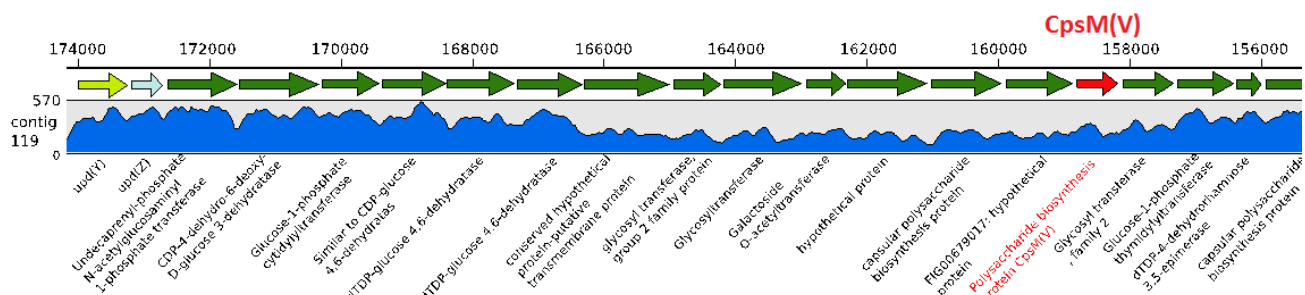


Figure 6: Illustration of the PSH, peg.1727 locus depicting the position of the virulence associated gene, CpsM (in red).

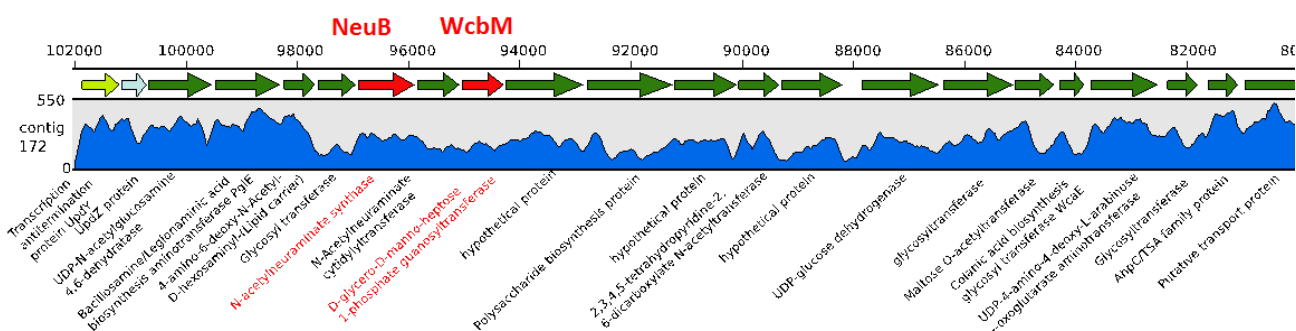


Figure 7: Illustration of the PSA, peg.2076 locus depicting the position of the virulence associated genes, NeuB and WcbM (in red).

While on the PSH locus (see figure 6) the gene sequence CpsM codes for a capsular polysaccharide protein facilitating transport, the PSA locus (see figure 7) contains two virulence associated gene sequences. WcbM codes for a D-glycero-D-mano-

heptose-1-phosphate guanosyltransferase, which is used in the translocation process across the outer membrane. The NeuB sequence codes for N-acetylneuraminate synthase and is part of the sialic acid synthesis. Since these three genes have been found in high abundance in inflamed pouches, further investigations were undertaken trying to knock out these virulence associated genes via a method called suicide vector mutagenesis in order to investigate their possible role in the pathogenesis of pouchitis.

1.3 Principle of suicide vector mutagenesis

The principle of suicide vector mutagenesis is based on allelic exchange by homologous recombination. For investigations in specific gene knock out mutants analysing their phenotype and function, allelic exchange has been used frequently. For studying the function of certain genes in the course of complex processes like pathogenesis, structure-functional interaction and vaccine production, it demands generating different mutant strains. To inactivate a specific gene, a suicide vector system is used which transfers the allele containing the wanted mutation or knock out into the host strain. Subsequently homologous recombination and assimilation of the mutated gene in the host genome lead to the identification of the mutants by means of selectable or counterselectable markers. These markers provide evidence of a successful integration by their response to sensitivity or resistance to chemical compounds or drugs (Ortiz-Martín, Macho, Lambersten, Ramos, & Beuzón, 2006; Reytrat, Pelicic, Gicquel, & Rappuoli, 1998; Zhou, Thompson, Xu, & Tiedje, 2004).

1.3.1 Suicide vector systems and counterselectable makers

Suicide vector systems are keystones in allelic exchange mutagenesis and have to show certain properties for a successful knock out gene integration into the chromosome. Suicide plasmids must possess the ability to replicate only in the tolerant host and contain a selectable marker allowing followed selection. As a last condition suicide plasmids should be applicable in multiple organisms to facilitate preferred conjugation as a transfer mechanism (Zhou et al., 2004). This mechanism sometimes

may be inefficient since double crossover events can be of low incidence or unwanted recombination events appeared. As a result the allelic exchange mutagenesis will lead to a small number of mutants and further isolation difficulties (Reyrat et al., 1998). Therefore counterselectable markers like sucrose, fusaric acid or streptomycin are incorporated into the suicide vector and drive death of the microorganism containing the counterselectable gene. Meaning the promotion of death of mutants which have undergone a successful transfer of the suicide vector (Reyrat et al., 1998; Zhou et al., 2004).

1.3.2 Principle of double-cross-over recombination in targeted suicide vector mutagenesis

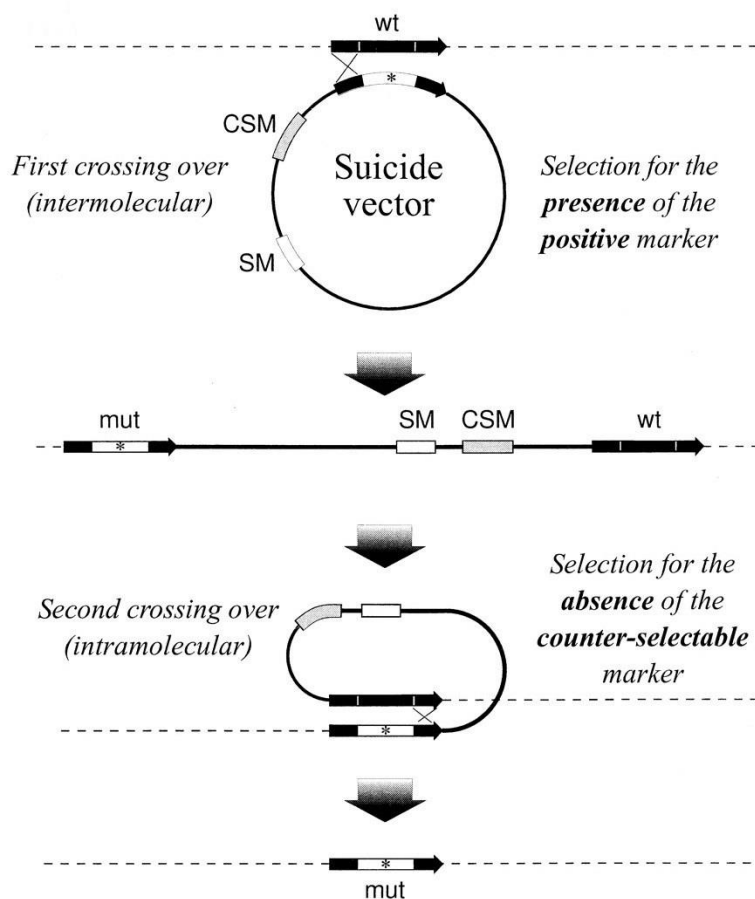


Figure 8: Principle of double-cross-over recombination. CSM, counterselectable marker; SM, selectable marker; WT, wild type allele; mut, mutated allele (Reyrat et al., 1998)

Double-cross-over recombination (see figure 8) targets allelic exchange associated gene inactivation. Thereby knockout mutants are generated through using counterselectable markers.

The double-cross-over recombination is a two-step procedure possessing the generation of certain unmarked mutants which contain small, hard detectable changes like in-frame deletions or point mutations. The first step comprises the integration of the suicide vector into the target mutated gene (wt) in the context of intermolecular recombination. These clones contain a selectable marker (SM), an antibiotic resistance cassette, and can therefore be selected by positive selection on antibiotic exposed medium. Positives are then cultured for the second cross-over event. The excision of the prior integrated suicide vector performed in the second cross-over event leads to strains containing the mutated gene (mut) and lost their suicide vector. By plating the culture on counterselectable medium, successful knockout mutants can be seen as negatives. Because the double-cross-over recombination comprises two intermolecular recombination events, the loss of the suicide vector can bring along both a mutant and a wild type phenotype (Ortiz-Martín et al., 2006; Reytrat et al., 1998; Zhou et al., 2004).

1.4 Thesis aim

Since the properties of *B. fragilis* have been investigated in a great extent in the past years, there is evidence that the microorganism might be involved in the pathogenesis of IBD. On this basis three different virulence associated genes have been found on the capsular polysaccharide loci of *B. fragilis*. The aim of the thesis is to demonstrate a way to generate an isogenic mutant by knocking out one antitermination factor, UpxY, a virulence associated gene (peg.1727), on the PSH locus and to confirm its successful deletion in the chromosome. In addition a competitive PCR assay between the peg.1727_psh isogenic mutant and wild type *B.fragilis* p207 and several assays, such as Biofilm formation and capsule staining assays, investigating the different phenotypes of both peg1727_psh and p207 will be made. This gives evidence about possible downstream effects of how the deleted gene sequence peg.1727 influences the virulent characteristics of *B. fragilis*.

2 Materials and Methods

2.1 Suicide vector mutagenesis

Table 1: List of primer sequences used in the course of the suicide vector mutagenesis

Primer name	Sequence
DR147 1kbP207peg1727S	5`-ATA GCG GGA TCC ATA GAT TTA TAA TCA AGT C-3`
DR148 1kbP207peg1727S	5`-GTC TGC TAT TTT ACT GTG TGA TCT CAA AAC CCT CCC C-3`
DR149 1kbP207peg1727 S	5`-G GGG AGG GTT TTG AGA TCA CAC AGT AAA ATA GCA GAC-3`
DR150 1kbP207peg1727S	5`-ATA GCG GGA TCC AGA CCG TAG AAG TTA TTG ATC C-3`
DR151 peg1727 test 1F	5`-CCG TAT CTA ATA TCT TCG TTC ATA GC-3`
DR152 peg1727 test 2F	5`-CAC TTA CAG CCG TGA GCT TG-3`
DR153 peg1727 test 1R	5`-CCA AGG TGT ACA AAG CGG TAA-3`

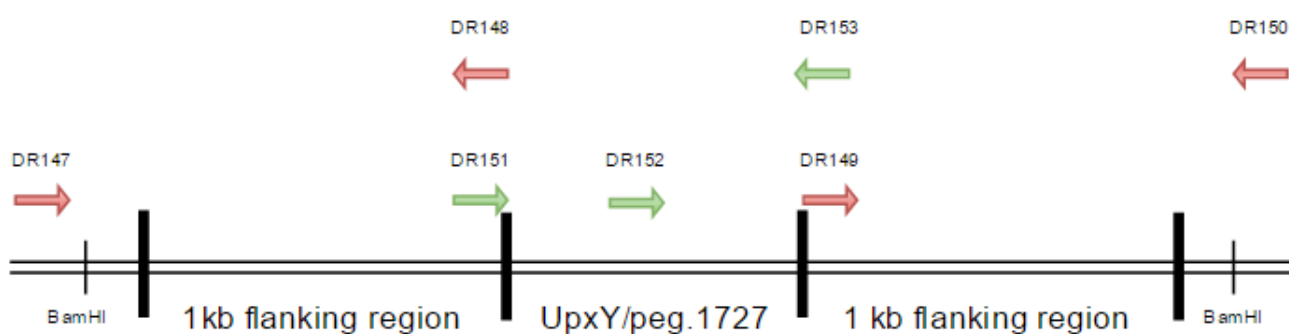


Figure 9: Illustration of the p207 gene sequence divided into the UpxY antitermination sequence, peg.1727, and its upstream and downstream flanking regions (1 kb in length). The arrows show the different primers used in the course of the suicide vector mutagenesis, namely DR147, DR148, DR149, DR150, DR151, DR152, DR153. The colors illustrate the paired primers.

Table 2: List of primer sequences used in qPCRs

Primer name	Sequence
DR168 P207uphY qPCR F	5`-TTGTGAAGGAATCCCCAGAG-3`
DR169 P207uphY qPCR R	5`-GACCGCAGGAACCAATTTAC-3`
DR119Bfrag16SqPCR618	5`-CAGTCTTGAGTACAG- TAGAGGTGG-3`
DR120Bfrag16SqPCR779	5`-GTGGACTACCAGGG- TATCTAATCC-3`
DR115 p207peg1740CpsMqPCR F	5`-TGATCAAGATATCCCCGTATCC-3`
DR116 p207peg1740CpsMqPCR R	5`-GAAGAACGATGGAACAGGAAAG- 3`

2.1.1 Fusion PCR

The first step is the polymerase chain reaction which amplified the two separate segments containing either the upstream or downstream 1kb flanking region plus a clamp sequence serving as an additional region for an improved polymerase alignment during the PCR. A BamHI restriction site was incorporated into the clamp sequence for the digestion and ligation process (see figure 9). For the amplification of the first segment primers DR147 1kbP207peg1727S 5`-ATA GCG GGA TCC ATA GAT TTA TAA TCA AGT C-3` and DR148 1kbP207peg1727S 5`-GTC TGC TAT TTT ACT GTG TGA TCT CAA AAC CCT CCC C-3` were used. To amplify the second segment primers DR149 1kbP207peg1727 S 5`-G GGG AGG GTT TTG AGA TCA CAC AGT AAA ATA GCA GAC-3` and DR150 1kbP207peg1727S 5`-ATA GCG GGA TCC AGA CCG TAG AAG TTA TTG ATC C-3` were used. The PCR reaction was set to the parameters listed in table 3.

Table 3: Polymerase Chain Reaction set up

3 min	95C	
30 sec	95C	
30 sec	60C	x35 cycles
1.5 min	72C	

10 min	72C
Indef	4C

After the two segments were amplified by PCR, these two fragments were fused together by overlap extension PCR. Primers DR147 1kbP207peg1727S 5`-ATA GCG GGA TCC ATA GAT TTA TAA TCA AGT C-3` and DR150 1kbP207peg1727S 5`-ATA GCG GGA TCC AGA CCG TAG AAG TTA TTG ATC C-3` were used for the fusion process. To increase the success rate the annealing temperature was set to 55°C. Through this method the sequence, peg.1727, in between of the two segments was deleted.

2.1.2 Plasmid purification

The plasmid pKnock-Erm (1,8kb, Addgene) was purified by using the QIAquick PCR Purification Kit (QIAGEN) under the instructions provided from the manufacturer. The final elution volume was set to 30 µl EB elution buffer to yield a higher concentration. The purified plasmid DNA was stored at -20°C until further use.

2.1.3 Digestion

The purified PCR product, peg.1727, and pKnock plasmid were digested in order to be able to be used in the followed ligation. 10x BamHI buffer and BamHI enzyme are supplied by New England Biolabs. Peg.1727 and pKnock were digested in two different tubes according to the table below (see Table 4).

Table 4: Digestion of peg.1727 and pKnock

	Peg.1727 [µl]	pKnock only [µl]
DNA	15	15
10x BamHI buffer	2	2
H₂O	2	2
BamHI	1	1
Total amount:	20	20

The digestion reaction was run for 2h at 37°C. After 1h 1µl of Calf Intestinal Alkaline Phosphatase (CIP) (New England Biolabs) was added to the pKnock only reaction

in order to dephosphorylate 5` and 3` end of the DNA phosphomonoesters and incubation for the remaining 1h was continued.

After the incubation the digestion products were loaded onto a 1% agarose gel and gel electrophoresis was run for 40 min. The wanted gene products of *peg.1727* and *pKnock* were visualized by UV in the High Performance UV Transilluminator (Kodak) and the gel area containing the corresponding bands were cut out. For *peg.1727* the sequence is 2000 kb long and *pKnock* contained 1,8 kb. The digested DNA enclosed in the gel, was extracted by QIAquick Gel Extraction Kit (QIAGEN) and finally eluted in 25 μ l of low salt - EB buffer.

2.1.4 Ligation

The extracted, digested samples were ligated using the following components indicated in Table 5. 10x buffer for T4 DNA Ligase and T4 DNA Ligase were supplied by New England Biolabs.

Table 5: Ligation of *pKnock* with *peg 1727* and *pKnock* only

	pKnock + <i>peg.1727</i> [μl]	pKnock only [μl]
cut pKnock	10	10
Cut <i>peg.1727</i>	7	-
H₂O	-	7
T4 Buffer	2	2
T4 enzyme	1	1
Total amount	20	20

The ligation reaction was incubated at room temperature (RT) for 2h and then stored at -20°C.

2.1.5 Transformation

5 μ l of either *pKnock+ peg.1727* or *pKnock* only were added to 50 μ l S17-1 *Escherichia coli* electrocompetent cells, containing 10^{10} cells. These mixtures were transferred into 0,4 cm electroporation cuvettes (BioRad) and then electrically pulsed using the Micropulser™ (BioRad) under 1.8 kV. Directly after the electric pulse 250 μ l S.O.C medium (Invitrogen) were added to each sample and incubated for 1h at 37°C

in a shaking incubator (New Brunswick Scientific). 300 µl of each sample were then plated out on one LB w/ampicillin plate (0,1% Amp) and incubated o/n at 37°C. Positive colonies were then inoculated in 5 ml LB w/ampicillin medium (0,1% Amp).

2.1.6 Control PCR

To confirm the successful transformation a control PCR was made. A dirty lysate was made by touching one colony, transfer it to 5 µl nuclease free water (Ambion) and microwave the tube for 2 min. The reagents (TaKaRa Ex taq) were used. A master mix containing 17,375 µl nuclease free water (Ambion), 2,5 µl 10x Ex Taq Buffer, 1 µl of each primer (0,5 µM) and 0,125 µl TaKaRa Ex Taq enzyme per run was prepared. 2 µl of each DNA was added to 23 µl of master mix into PCR tubes. A negative and a positive control (genomic DNA of p207) was implemented beside the *peg.1727_psh* mutant. Using the BioRad Thermocycler, the programme was set to denaturation at 95°C for 3 min, followed by 35 amplification cycles of denaturation at 95°C for 30s, primer annealing at 60°C for 30s, extension at 72°C for 1,5 min and a final extension step at 72°C for 10 min. The incubation is hold indefinitely at 4°C until gel electrophoresis as started-

2.1.7 Conjugation into *Bacteroides fragilis*

5 ml cultures of S17-1_pKnock_peg.1727 in LB w/0,1% Amp, helper Plasmid RK 231 in LB w/0,1% Kanamycin (Kan) and *B. fragilis strain* p207 in BHIS medium were inoculated o/n. The next day 100 µl of p207 were passaged into new BHIS medium and grown to end of log-phase with an OD600 between 0,5 and 1.

2 ml of each three strains were pipetted into two separate tubes, centrifuged at 10000 rpm for 5 min, 500 µl of BHIS were added and centrifuged at 10000 rpm for 5 min. The cultures were vortexed and S17-1_pKnock_peg.1727, RK 231 and *B. fragilis* p207 were poured together. Then the whole amount of the mixed cultures was plated as one big drop on center of a BHIS plate and incubated anaerobic o/n.

One tube with 500 µl BHIS per conjugation was prepared and the grown lawn was resuspended by vortexing. 160 µl of the resuspended culture was plated on BHIS

w/clindamycin + gentamicin plates (concentration of 5 µg/ml) and incubated anaerobic for 2-3 days until colonies are visible. Positive colonies represented *B. fragilis* p207 bacteria which have incorporated the ligated pKnock_peg.1727 plasmid and were inoculated in BHIS medium.

2.1.8 Passage and screening patch

To screen for colonies which have incorporated only the deletion construct peg.1727 into their chromosome, 50 µl of the o/n culture was plated out on BHIS plates and incubated anaerobic at 37°C for 48 h. Single colonies were then simultaneously patched once on a Brain Heart Infusion supplemented (BHIS) plate and once on a BHIS w/clindamycin plate 100-fold. After 48 h of anaerobic incubation at 37°C, patches were screened for negatives on the BHIS w/clindamycin plates and corresponding positives on the BHIS plates. These colonies have undergone a successful crossing over at the chromosomal level and represented successful mutants. For later use the mutated colonies were grown anaerobic o/n at 37°C and then frozen down in 0,25% glycerol at -80°C.

2.2 Downstream suicide vector mutagenesis confirmation methods

2.2.1 DNA extraction and purification

Peg.1727_psh mutant was grown anaerobic in brain heart infusion supplemented (BHIS) broth composed of 37 g/l BHI (Becton Dickinson, Sparks, MD), 5 g/l Yeast Extract (Fisher Scientific), 0,5 g/l L-Cysteine (Sigma), 10 ml/l 0.01% Vitamin K, 5 mg/l hemin. For BHIS plates additional 15 g/l Difco™ Agar, Granulated (Becton Dickinson, Sparks, MD) was added. A 5 ml aliquot of the o/n culture was spin down at 5000 rpm for 10 min at 4°C. The supernatant was discharged and the pellet processed using the DNeasy Blood & Tissue Kit (QIAGEN) under the instructions provided from the manufacturer. The final purified DNA was stored at -20°C until further use.

2.2.2 RNA isolation

Peg.1727_psh mutant was grown o/n in BHIS broth and a 2 ml aliquot was spin down at 5000 rpm for 10 min at 4°C. The supernatant was discharged, the pellet resuspended in 250 µl RNa protect Bacteria Reagent (QIAGEN) and stored in -80°C until further use. RNA was then isolated using the Kit ZR Soil/Fecal RNA Micro-Prep™ (Zymo Research) under the instructions provided from the manufacturer.

2.2.3 cDNA synthesis

The concentration of the extracted RNA was measured using the NanoDrop Lite (Thermo Scientific) and diluted in Nuclease Free Water (Ambion) to contain 1 µg/10 µl total RNA. Using the Transcriptor First Strand cDNA Synthesis Kit (Roche) reverse transcription was performed. Upon the recommendation of the manufacturer the optional step using anchored-oligo (dT) primer and random hexamer primer was performed. For denaturation of the RNA 1 µl of anchored-oligo (dT) primer and 2 µl of random hexamer primer were added to the PCR tube and heated at 65°C for 10 min in the BioRad Thermocycler. The remaining components consisting of 4 µl 5x Reaction buffer, 0,5 µl RNase inhibitor, 2 µl dNTPs and 0,5 µl reverse transcriptase were added and Real Time (RT) reaction was started using the BioRad Thermocycler. The program was set to 10 min at 25°C, followed by 30 min at 55°C, 10 min at 85°C and infinity hold at 4°C. cDNA synthesized samples were stored at -20°C until further use.

2.2.4 PCR

Peg.1727_psh mutant was grown 48h anaerobic on brain heart infusion supplemented (BHIS) plates. A dirty lysate was made by touching one colony, transfer it to 5 µl nuclease free water (Ambion) and microwave the tube for 2 min. The reagents (TaKaRa Ex taq) were used. A master mix containing 17,375 µl nuclease free water (Ambion), 2,5 µl 10x Ex Taq Buffer, 1 µl of each primer (0,5 µM) (see table 1) and 0,125 µl TaKaRa Ex Taq enzyme per run was prepared. 2 µl of each DNA was added to 23 µl of master mix into PCR tubes. A negative and a positive control (genomic DNA of p207) was implemented beside the peg.1727_psh mutant. Using

the BioRad Thermocycler, the programme was set to denaturation at 95°C for 3 min, followed by 35 amplification cycles of denaturation at 95°C for 30s, primer annealing at 60°C for 30s, extension at 72°C for 1,5 min and a final extension step at 72°C for 10 min. The incubation is hold indefinitely at 4°C until further use.

2.2.5 Agarose gel electrophoresis

A 1% agarose gel was made by dissolving 0,5 g of Quick dissolve agarose (Gene Mate) in 50 ml TBE buffer and boiling until solution was completely homogenized. Then 3 µl of ethidium bromide (1% Solution, Fisher Bioreagents) were added to the solution. The solution was poured in a horizontal gel chamber and cooled at room temperature for 35 min until gel was solidified. Followed the gel was covered by TBE buffer. After adding 1 µl of 6x loading dye (New England Biolabs) to 5 µl of PCR sample, 5 µl of each sample and an appropriate DNA ladder (New England Biolabs) were loaded in a well. For the separation a voltage of 110 Volt was applied. The resulting bands were visualized by High Performance UV Transilluminator (Kodak).

2.2.6 ExoSAP-IT PCR Cleanup

The ExoSAP-IT PCR Cleanup (Affymetrix) is an enzymatic cleanup of PCR products and eliminates contaminating primers and dNTPs. To 5 µl of the post-PCR reaction product 2 µl of ExoSAP-IT reagent (Affymetrix) is added. Incubate at 37°C for 15 min for degrading remaining nucleotides and primers and then incubate at 80°C for 15 min in order to inactivate the ExoSAP-IT reagent. The PCR product was then submitted for sequencing.

2.2.7 RT-qPCR

A master mix of total 35 µl/well was prepared containing 14 µl of nuclease free water (Ambion), 17,5 µl Sybr Green (BioRad), 1,75 µl forward and reverse primer each (10µM working stock concentration). Using a round bottom 96-well plate (Sigma Aldrich) 2,5 µl/well of sample cDNA is added, giving a total volume of 37,5 µl. Centrifuge at 1500 rpm for 1 min at 4°C. One sample was plated out in triplicates of 10 µl

each in a clear, flat bottom 384-well plate (Sigma Aldrich) and covered with a Mi-cro-seal® B adhesive sealer (Biorad). Centrifuge at 1500 rpm for 1 min at 4°C. 384-well plate was then analyzed in Light Cycler (Roche). Programme was set to pre-incubation at 95°C for 5 min, followed by 45 amplification cycles of 95°C for 10s, 56°C for 20s, 72 for 30s, followed by a melting curve of 95°C for 5 s, 65°C for 1 min and cooling for 10 s at 40°C.

2.3 Competitive qPCR assay between peg.1727_psh mutant and P207

2.3.1 Growth curve and calculation for CFU/ml of peg.1727_psh mutant and p207

Crystals of p207 and peg.1727 were streaked out directly from the glycerol stock on BHIS plates and incubated at 37°C under anaerobic conditions for 48h. One single colony was inoculated in fresh BHIS medium and incubated at 37°C under anaerobic conditions o/n. 3 replicates of 200 µl of each strain were inoculated into 10 ml of BHIS. The OD600 was checked before and adjusted to the same OD if necessary. The OD600 was then measured in disposable plastic cuvettes (Fisher Scientific) every hour for 11 time points using Spectronic™ 200 Spectrophotometer (Thermo Scientific). As soon as the cultures reached an OD of 0,5, 100 µl of the both strains cultures were transferred into 900 ml of pre-reduced PBS. Then the culture was serially diluted in a 1/10 ratio up to 10⁻⁷ and 100 µl µl of dilutions 10⁻⁶, 10⁻⁷ were plated out in duplicates on BHIS plates. The plates were incubated for 48h at 37°C anaerobically and the grown colonies counted. For further use both cultures were divided into 2 ml aliquots and spin down at 8000 rpm at 4°C for 10 min. The pellet was stored at -20°C for later use. Based on the colony counts, the CFU/ml for p207 and peg.1727 were calculated.

2.3.2 Competition assay

Based on the calculation of the CFU/ml, 100 µl of p207 and peg.1727 culture with a target of 10⁹ CFU/ml at an OD of 0,5 were inoculated into fresh, pre-warmed BHIS

media. 1 ml aliquots were removed at 4 different time points (t=0h, 2h, 4h, 6h) into bead-beating tubes (Fisher Scientific) and stored at -20°C.

2.3.3 DNA extraction

After frozen samples (from 2.3.2) were thawed, 1 ml of lysis buffer and 20 µl proteinase K (20 mg/ml) were added to each tube. To lyse and disrupt the microbial cells the bead-beating tubes were processed for 5 min in a Mini-Beadbeater-8k Cell Disrupter (BioSpec Products). The samples were incubated for 4h at 55°C in shaking water bath. The tubes were shortly spin down and 600 µl of the supernatant were transferred to another 1,5 ml eppendorf (Fisher Scientific) tube. 600 µl of phenol:chloroform:isoamylalcohol+Tris (25:24:1, Ambion) were added to each tube, mixed for 30 seconds and centrifuged at maximum speed for 5 min at RT. 450 µl of the top phase were transferred into a new 1,5 ml Eppendorf tube, an equal amount (450 µl) of chloroform were added, mixed for 30 seconds and centrifuged at maximum speed for 5 min at RT. 450 µl of the top phase were transferred into a new 1,5 ml Eppendorf tube, an equal amount (450 µl) of 100% isopropanol were added, mixed by inverting tube and stored at -20°C for 30 min to precipitate the DNA. Then the tubes were spin down at 4°C at max speed for 5 min to pellet DNA. Excess was dumped out and the pellet was washed with 400 µl 70% ethanol. After a quick spin, supernatant was dumped out and the residual 70% ethanol excess was removed with a pipet. The tubes, with caps open, were then placed in an Isotemp™ heating block (Fisher Scientific) at 55°C for 45 min and then resuspended in 30 µl of nuclease free water (Ambion). Closed tubes were placed in 55°C Isotemp™ heating block (Fisher Scientific) for 30 min to ensure that DNA was dissolved and stored at -20°C until further use.

The DNA was quantified to reach a dilution of 20-30 ng/µl by the using the ds DNA HS (High Sensitivity) assay kit through the Qubit Fluorometer (Invitrogen). The DNA was quantified under the instructions provided from the manufacturer. The final diluted DNA was stored at -80°C until further use.

2.3.4 qPCR Evaluation

Two mastermixes were prepared using the following components indicated in Table 6. One mastermix contained the 16S primers, DR119Bfrag16SqPCR618 5`-CAG-TCTTGAGTACAGTAGAGGTGG-3` and DR120Bfrag16SqPCR779 5`-GTGGAC-TACCAGGGTATCTAATCC-3`, while the other mastermix contained the UphY primers, DR168 P207uphY qPCR F 5`-TTGTGAAGGAATCCCCAGAG-3` and DR169 P207uphY qPCR R 5`-GACCGCAGGAACCAATTTAC-3`.

Table 6: components of qPCR mastermix

	Amount for 1 run [μ l]
Sybr green mastermix (2x)	10
Primer forward	0,1
Primer reverse	0,1
dH₂O	7,8
DNA	2
Total amount:	20

The samples were loaded in duplicates in a 384 plate. Additionally a serially dilution to 10^{-5} of mid-log phase p207 DNA was incorporated into the analysis and loaded in the 384 plate, too. The qPCR was set for a 5 min incubation time at 94°C followed by 40 cycles of amplifications, each of 5 seconds at 94°C and 30 seconds at 60°C and a subsequent cooling step.

2.4 Biofilm formation assay

5 replicons of 200 μ l of p207 Δ 1727 (mutant strain), p207 (human isolate strain), P214 (additional human isolate strain) and 9343 (reference strain) culture and BHI medium only were put each into a single well in a round bottom 96-well plate (Sigma Aldrich). The plate was incubated anaerobically at 37°C o/n. Then the culture was aspirated and gently washed two times with water. To each treated well 200 μ l of 0,1% Crystal Violet Solution (Sigma) was added and incubated at RT for 15 min. The Crystal Violet Solution was aspirated and the plate was washed two times with water to get rid of the excess solution. Then 200 μ l of 95% Ethanol (Decon Labs)

was added to each treated well and the plate was read at a wavelength of 550nm using the VERSAmax microplate reader (Molecular Devices).

The four strain cultures were exposed to three different bile acids. Sodium cholate hydrate (CA), Taurocholic acid sodium salt (TCA) and sodium deoxycholate (DCA) were used in a 0,15% final concentration dissolved in nanopure water (1,5 mg/ml). Strains were grown anaerobically at 37°C to mid log phase (OD=0,4) in a 50 ml culture tube and then exposed with 50 µl of the individual bile acid. 5 replicons of 200 µl of the four strains were directly put into a single well in a round bottom 96-well plate and incubated for 60 min in anaerobic conditions at 37°C. After exposure the previously described method was carried out.

2.5 Mandeval's capsule stain

30 µl of 1% Congo Red Solution (Carolina Biological Supply) was plated on a clean microscopic slide (Fisher Scientific) and then mixed with either 10 µl of the peg.1727 mutant strain culture or p207 strain culture and gently spread to form a smear. The suspension was air dried. Mandeval's solution (Carolina Biological Supply) was applied in drops on the slide covering the smear and let sit for 5 min. The excess stain was poured off and washed by dipping it into a water bath. The stained slide was then examined with an oil immersion at 1000x magnification using Leica DM2500 M microscope.

3 Results

3.1 Suicide vector mutagenesis

In the progress of the allelic exchange mutagenesis by a double cross-over event to generate a mutant of the *B.fragilis* strain p207, which misses a virulence associated gene sequence, *peg,1727*, certain confirmatory PCR gel electrophoresis have been performed. The gene sequence *peg.1727* is located on the PSH locus and regulates the transcription of *CpsM*, a capsular polysaccharide protein facilitating transport. The *peg.1727* locus is called *UpxY*, an antitermination factor, regulating the downstream *CpsM* biosynthesis (see Figure 5). By running several PCR gel electrophoresis we confirmed successful steps in the progress of generating the isogenic mutant. Genome sequencing was conducted to ensure the knockout of *Peg.1727* on a genomic level. Figure 9 illustrates all primers used in the course of the suicide vector mutagenesis.

3.1.1 PCR segments

As a first step the segment 1 and 2 were amplified using ones the set of DR147 1kbP207peg1727S 5`-ATA GCG GGA TCC ATA GAT TTA TAA TCA AGT C-3` and DR148 1kbP207peg1727S 5`-GTC TGC TAT TTT ACT GTG TGA TCT CAA AAC CCT CCC C-3` and the set of DR149 1kbP207peg1727 S 5`-G GGG AGG GTT TTG AGA TCA CAC AGT AAA ATA GCA GAC-3` and DR150 1kbP207peg1727S 5`-ATA GCG GGA TCC AGA CCG TAG AAG TTA TTG ATC C-3. After the PCR cycle the two PCR products were loaded into wells, segment 1 in wells 3/4 and segment 2 in wells 6/7. Additional a 1kb DNA ladder in well 1 and a negative control for each segment in wells 2/5 were loaded and the gel electrophoresis was started.

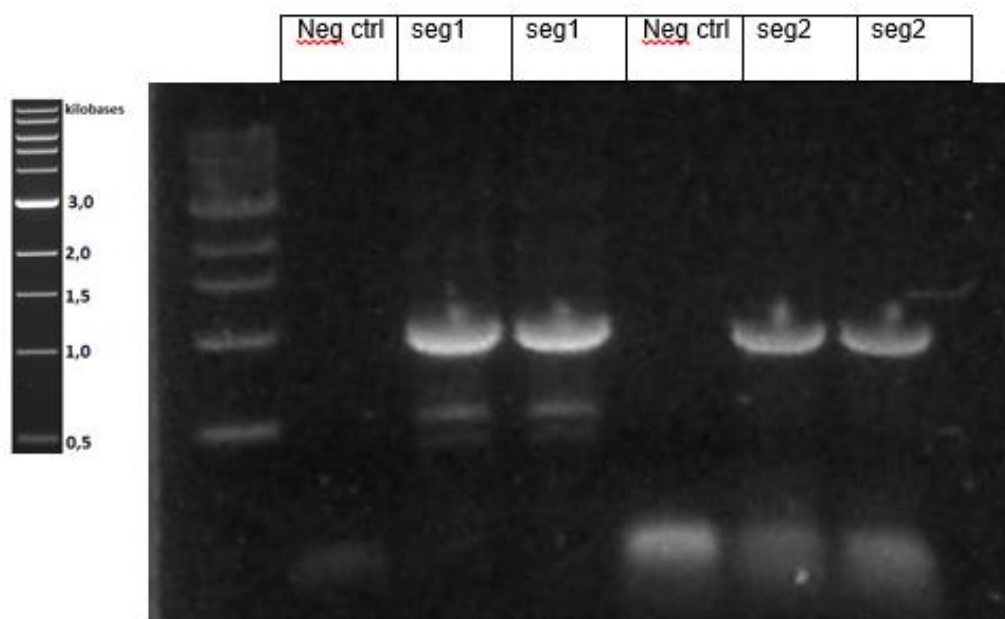


Figure 10: Gel electrophoresis confirming generation of segments 1 and 2 of p207 peg1727 gene for mutant construction. For segment 1 DR147 and DR148 primers were used, whereas for segment 2 DR149 and DR150 were used. The 1 kb DNA ladder on the left (500 µg/ml, New England Biolabs) was chosen as a reference. The negative controls (neg ctrl) was made of Master Mix only. In well 3 and 4 two sets of segment 1 and in well 6 and 7 two sets of segment 2 were loaded.

The successful generation of the two segments is shown in Figure 10. Both in wells 3/4 and in wells 6/7 containing one of the segments, bands at 1000 bp were found. This confirms the successful segment construction. The light bands on the bottom of the gel represent primer dimers.

3.1.2 Confirmatory Fusion PCR

After the two separate amplifications of segment 1 and 2, these two fragments were fused together by overlap extension PCR. Through this method the sequence in between of the two segments was deleted. To confirm a successful fusion a PCR using DR147 1kbP207peg1727S 5`-ATA GCG GGA TCC ATA GAT TTA TAA TCA AGT C-3` and DR150 1kbP207peg1727S 5`-ATA GCG GGA TCC AGA CCG TAG AAG TTA TTG ATC C-3` primers was conducted. DR147 sits on the 5` end of the upstream flanking region and DR150 sits on the 3` end of the downstream flanking region. To increase the success rate the annealing temperature was increased to 55°C. Two sets of mixed segment 1 and segment 2 (well 2 and 3) and a negative

control of Master Mix only (well 1) were loaded into the wells and the gel electrophoresis was started.

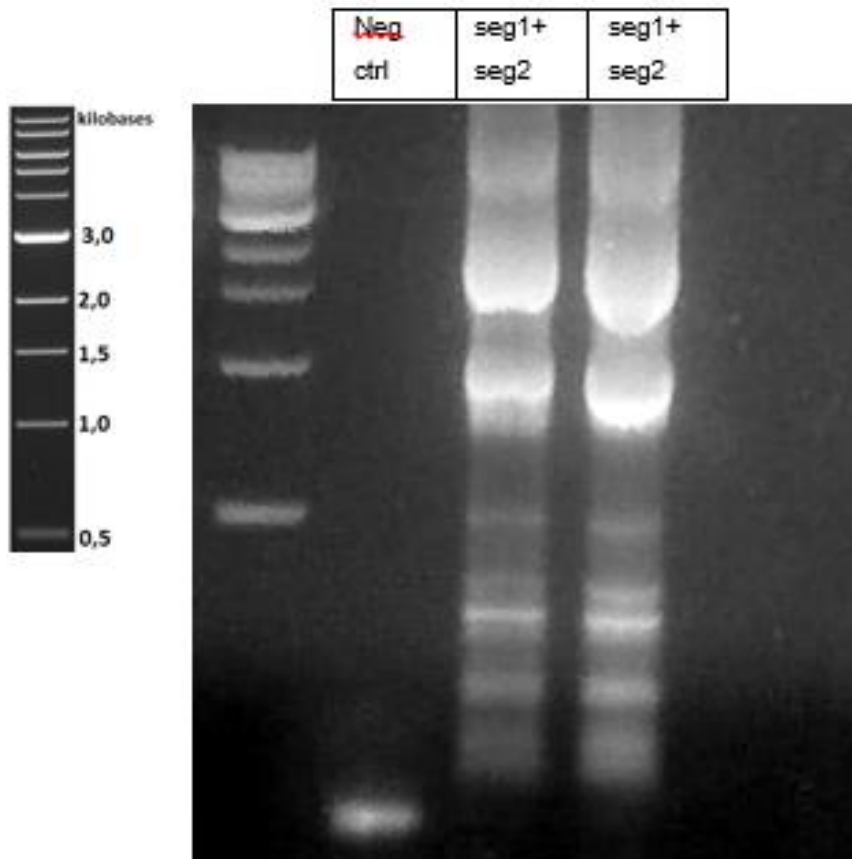


Figure 11: Gel electrophoresis confirming the fusion of segments 1 and 2 of p207 peg1727 gene for mutant construction using DR147 and DR150 primers. The 1 kb DNA ladder on the left (500 µg/ml, New England Biolabs) was chosen as a reference. The negative control (neg ctrl) was made of Master Mix only. In well 3 and 4 two sets of mixed segment 1 and segment 2 (seg1+seg2) were loaded.

The successful fusion of the two segments is shown in Figure 11. In both wells containing the mixed two segments, a band at 2000 bp was found. This confirms the successful fused PCR construct missing peg.1727 sequence. The other bands are unfused 1kb flanking regions and primer dimers.

3.1.3 Confirmatory transformation PCR

After the fused PCR product was digested with BamHI restriction enzyme and ligated into the plasmid pKnock by T4 DNA Ligase a confirmatory PCR gel electrophoresis was run in order to verify the successful integration of the deletion construct, peg.1727, into pKnock in competent E.coli S17-1 cells. Thereby DR151 peg1727 test 1F with 5`-CCG TAT CTA ATA TCT TCG TTC ATA GC-3` and DR153 peg1727 test 1R with 5`-CCA AGG TGT ACA AAG CGG TAA-3` were used as these primers sit on the flanking regions upstream and downstream the deletion construct, peg.1727. A dirty lysate of 5 positive screened colonies, picked from a LB+Amp plate (well 3-7), as well as a 100 bp DNA ladder (well 1), a 1 kb DNA ladder (well 2), a negative control of Master Mix only (well 8) and a positive control of p207 genomic DNA (well 9) was analyzed.

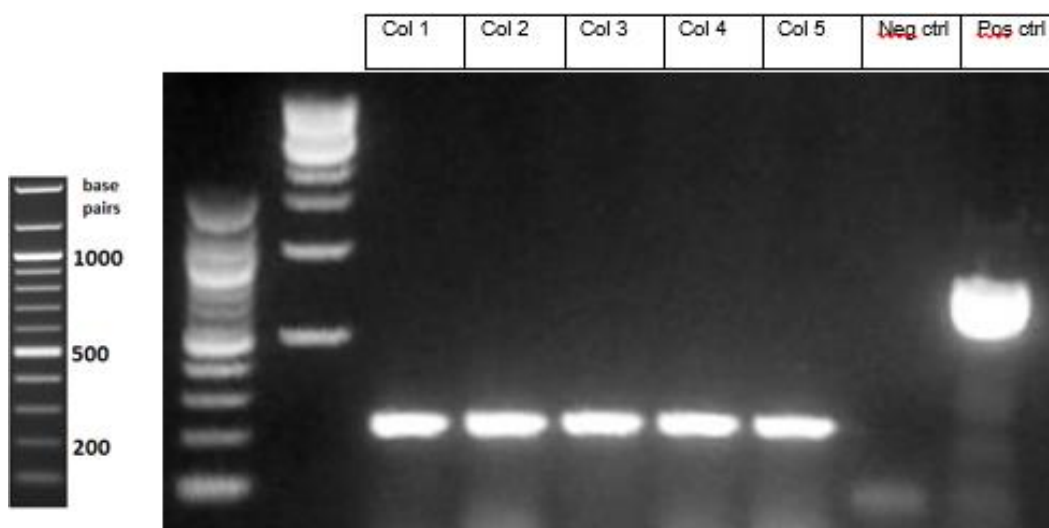


Figure 12: Gel electrophoresis confirming the insertion of the deletion construct peg.1727 into plasmid pKnock in competent E.coli 217-1 cells using DR151 and DR153 primers. The 100 bp DNA ladder and 1 kb DNA ladder (500 µg/ml, New England Biolabs) (well 1 and 2) were chosen as a reference. A dirty lysate of five different positive screened colonies, depicting potential transformed competent E.coli S17-1 cells with the incorporated peg.1727 in plasmid pKnock, was performed and loaded in wells Col1-Col5 (well 3-7). The negative control (neg ctrl) (well 8) was made of Master Mix only and the genomic DNA of p207 served as the positive control (pos ctrl) (well 9).

The successful insertion of the deletion construct, peg.1727, into plasmid pKnock in competent E.coli S17-1 cells is shown in Figure 12. All 5 screened colonies show the successful integration since their DNA fragment migrated to the band of 200 bp

compared to the genomic DNA of p207 at 1000 bp. The light bands on the bottom of the gel represent primer dimers.

3.1.4 Confirmatory mutagenesis PCR of peg.1727 into B.fragilis P207

S17-1_pKnock_peg.1727, RK 231 and *B. fragilis* p207 were conjugated and positive colonies selected (see 2.1.7). After the conjugation of S17-1_pKnock_peg.1727, RK 231 and *B. fragilis* p207, a PCR gel electrophoresis was performed confirming the successful insertion of the deletion construct, peg.1727, into the chromosome of *B.fragilis* p207. Potential mutants were screened before by patches on both counterselectable medium, BHIS+clindamycin, as well as on BHIS only medium. Colonies which were seen as negatives on the counterselectable medium and positives in the BHIS medium were potential mutants and tested for successful mutagenesis by PCR gel electrophoresis. Thereby once the primer set of DR151 peg1727 test 1F with 5`-CCG TAT CTA ATA TCT TCG TTC ATA GC-3` and DR153 peg1727 test 1R with 5`-CCA AGG TGT ACA AAG CGG TAA-3` were used as these primers sit on the flanking regions upstream and downstream of the deletion construct, peg.1727. Additional the primer set of DR151 peg1727 test 1F with 5`-CCG TAT CTA ATA TCT TCG TTC ATA GC-3` and DR152 peg1727 test 2F with 5`-CAC TTA CAG CCG TGA GCT TG-3` were used to demonstrate no amplification in the mutant as the sequence of DR152 is located on the deletion construct itself. A dirty lysate of the positive screened colonies on the BHIS plate (well 3 and 6), as well as a 100 bp DNA ladder (well 1), a negative control of Master Mix only (well 2 and 5) and a positive control of p207 genomic DNA (well 4 and 7) were loaded into the wells and the gel electrophoresis was started.

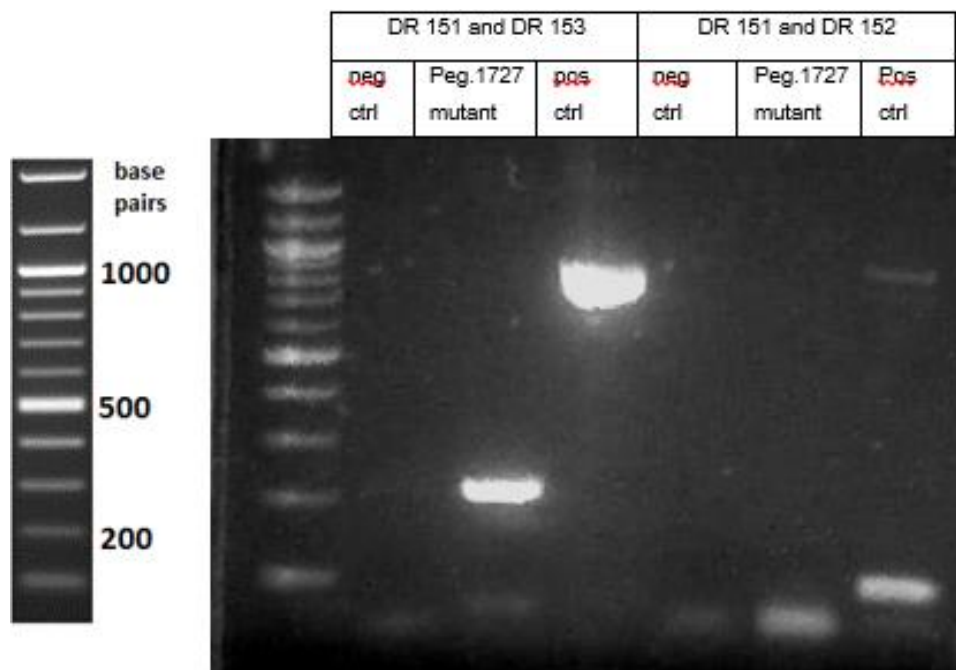


Figure 13: Gel electrophoresis confirming the insertion of the deletion construct *peg.1727* into *B.fragilis* *p207* using once the set of DR151 and DR153 primers as well as the set of DR151 and DR152. The 100 bp DNA ladder (500 µg/ml, New England Biolabs) (well 1) was chosen as a reference. A dirty lysate of the positive screened colony of a potential mutated *B.fragilis* undergone the crossover leading to the incorporation of *peg1727* into its chromosome, was performed and loaded into two wells named “Peg.1727 mutant” (well 3 and 6). The negative control (*neg ctrl*) (well 2 and 5) was made of Master Mix only and the genomic DNA of *p207* served as the positive control (*pos ctrl*) (well 4 and 7).

The successful insertion of the deletion construct, *peg.1727*, into *B.fragilis* *p207* by suicide vector mutagenesis is shown in Figure 13. In the first primer set of DR 151 and DR 153 the mutant showed a PCR product at 200 bp compared to the genomic DNA of *p207* at 1000 bp confirming the deletion of *peg.1727* in the genome. The second primer set of DR151 and DR152 showed no bands in the *peg.1727* mutant and a very short fragment of 100 bp for *p207*. This confirms the insertion of the deletion construct, as DR152 is located in the deleted sequence *peg.1727*.

3.1.5 Confirmatory mutagenesis qPCR of downstream gene sequence *peg.1740* expression

For additional confirmation that the *peg.1727* gene sequence has been successfully knocked out in the suicide vector mutagenesis, a qPCR was performed. Thereby DR115 *p207peg1740CpsMqPCR*F with 5`-TGATCAAGATATCCCCGTATCC-3`

and DR116 p207peg1740CpsMqPCR with 5`-GAAGAACGATGGAACAG-GAAAG-3` were used. This qPCR shows the expression of the downstream gene sequence, peg.1740, in the p207 WT and the peg.1727_psh mutant. It clearly depicts the successful deletion of the peg.1727 sequence since there is a very low expression in the isogenic mutant and a significantly higher expression in the WT.

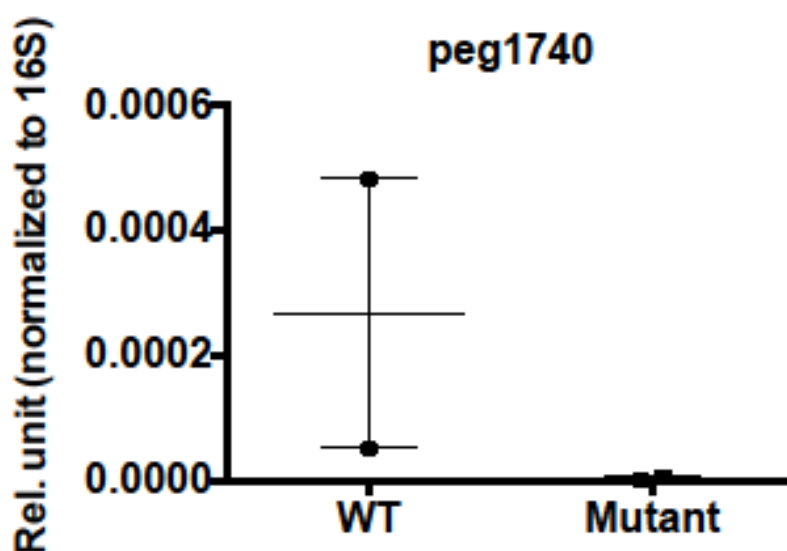


Figure 14: graphic illustration of the expression of peg 1740, a gene downstream of 1727, in the p207 WT strain (WT) and peg.1727_psh mutant (Mutant). The values are normalized to 16 S and depicted as relative units.

3.2 Transmission electron microscopy of peg.1727_psh and p207

For a phenotypic evaluation of the p207 wild type and the generated peg.1727_psh mutant a transmission electron microscopy (TEM) was performed. The handling of the TEM was undertaken by my supervisor Emma Liechty. Having a look on figure 15 no significant differences between the phenotypic appearances of p207 (A) and peg.1727_psh (B) can be seen. Both show the similar set up made up of the capsule, plasma membrane and cytosol (exterior to interior). The differences in size evolve as the picture were taken as cross sections of the individual bacterium. Because of the 3D nature of bacteria the picture could have been taken at different segments. All in all the images give evidence that there is no difference in growth morphology between the wild type and the isogenic mutant.

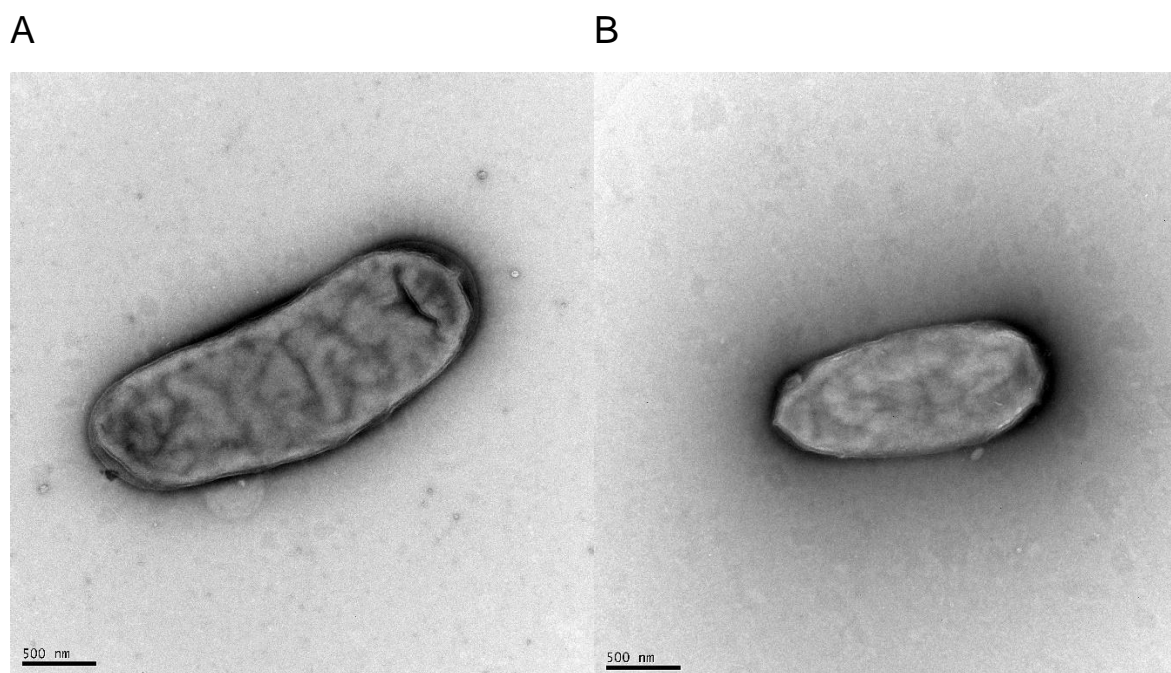


Figure 15: Transmission electron microscopy images of p207 (A) and peg.1727_psh (B)

3.3 Competitive qPCR assay between peg.1727_psh mutant and p207

For the analysis of the competitive qPCR several steps were undertaken. In order to provide the same CFU/ml of p207 and peg.1727, which are competing each other during the 6 hour assay, first growth characteristics were measured. Based on these measurements the appropriate amount of each culture was calculated. The ratio between a housekeeping gene, 16S, and the specific UpxY gene, which can only be found in the wild type strain p207, then was analyzed using qPCR.

3.3.1 Growth characteristics of peg.1727_psh and p207

OD 600 was measured at 11 time points. Based on OD measurements the mean values of both strains, p207 and peg.1727_psh were plotted against each other to illustrate their specific growth characteristics (see figure 17).

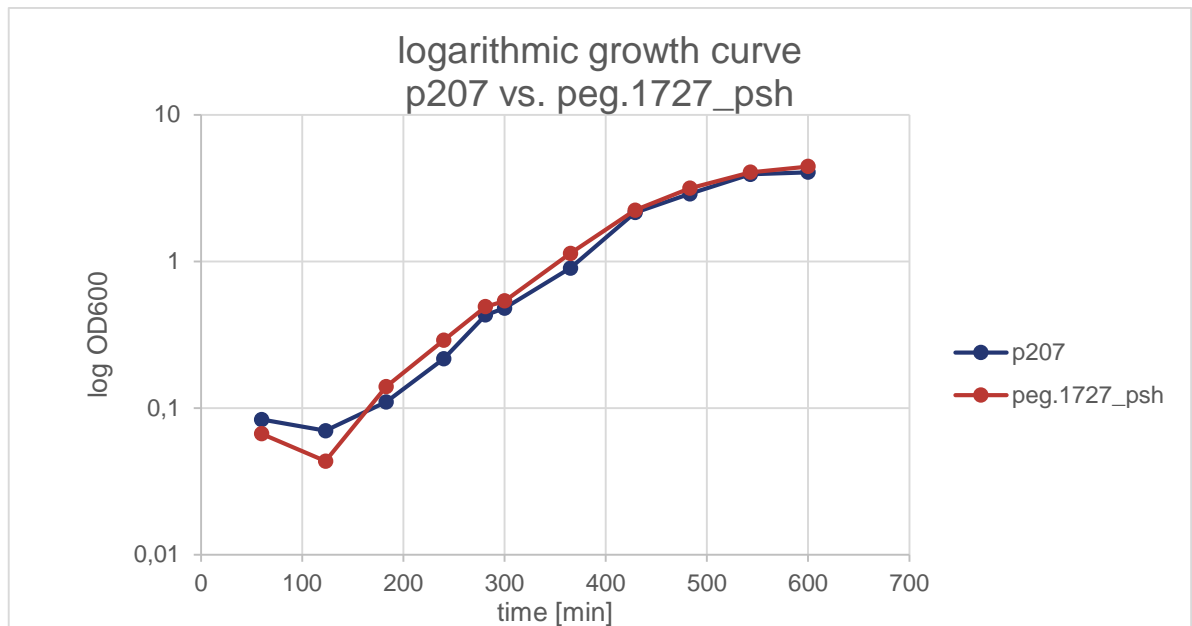


Figure 16: graphic illustration of the growth characteristics between *B.fragilis* p207 and *peg.1727_psh* in a logarithmic scale

3.3.2 Competitive qPCR assay

A competitive qPCR assay was performed to determine the relative abundance of the *peg.1727_psh* isogenic mutant to the wild type (WT) strain p207. In Figure 18 the abundance of the mutant is depicted as the ratio of the 10-power of obtained *peg.1727* normalized genomic copy numbers to the 10-power of the obtained WT normalized genomic copy numbers. These calculated ratios are standardized to the mean and plotted against the time period of 6 hours.

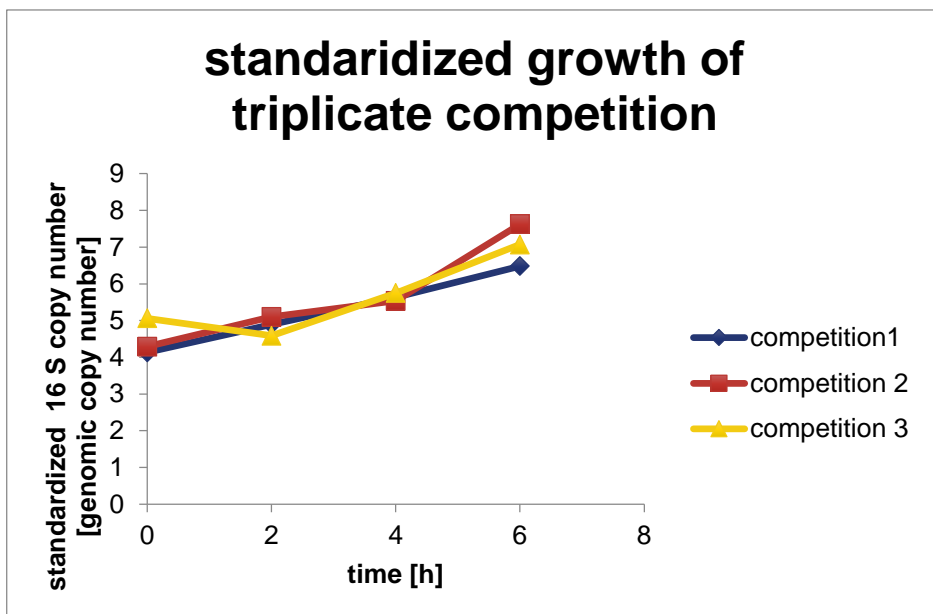


Figure 17: Illustration of the growth of the competition cultures 1, 2 and 3 in a standardized manner by means of a standard curve over the time period of 6 hours.

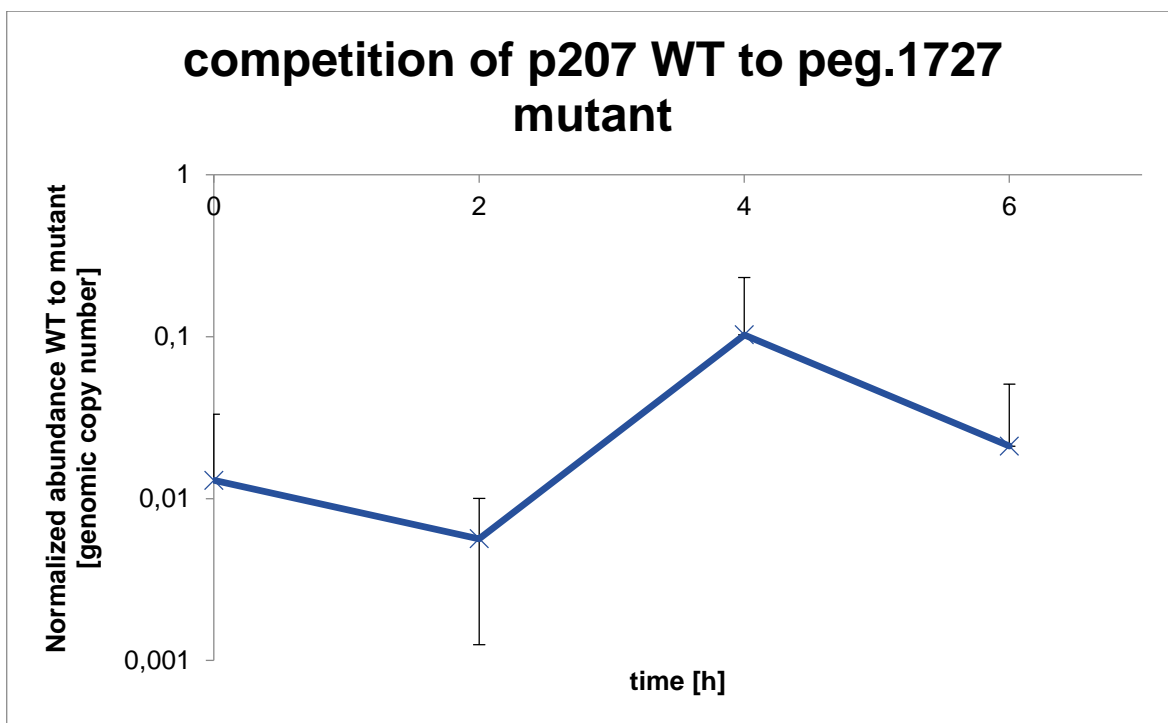


Figure 18: Competition assay between peg.1727 mutant and p207 WT strain. The depicted values are obtained as a standardized mean from three identical runs. In each time point ($t=0,2,4,6$) the relative population sizes of the peg.1727 mutant and the p207 WT strain are shown. The error bars represent the standard deviation by means of the triplicate assay set up.

Analyzing the data via a one-way-ANOVA (Prism) there were no significant differences in all four different time points regarding the normalized abundance of the WT to the isogenic mutant.

3.4 Biofilm formation assay

The biofilm formation assay was performed to investigate the different extent of biofilm formation of the individual strains and the effect of bile acid exposure. The absorbance at 550 nm is directly proportional to the biofilm formed during the assay. The bile acid Sodium cholate hydrate (CA as a primary,), Taurocholic acid sodium salt (TCA) and sodium deoxycholate (DCA) as secondary bile acids were chosen as representatives of prevalent bile acids in the gut.

In figure 19 the absorbance at 550 nm of the human isolate p207, the psh mutant strain p207 Δ 1727, the human isolate p214, the reference strain 9343 and BHI medium only is depicted after anaerobic o/n incubation at 37°C. In figure 20 the absorbance at 550 nm of all four strains each exposed to three different bile acids is shown.

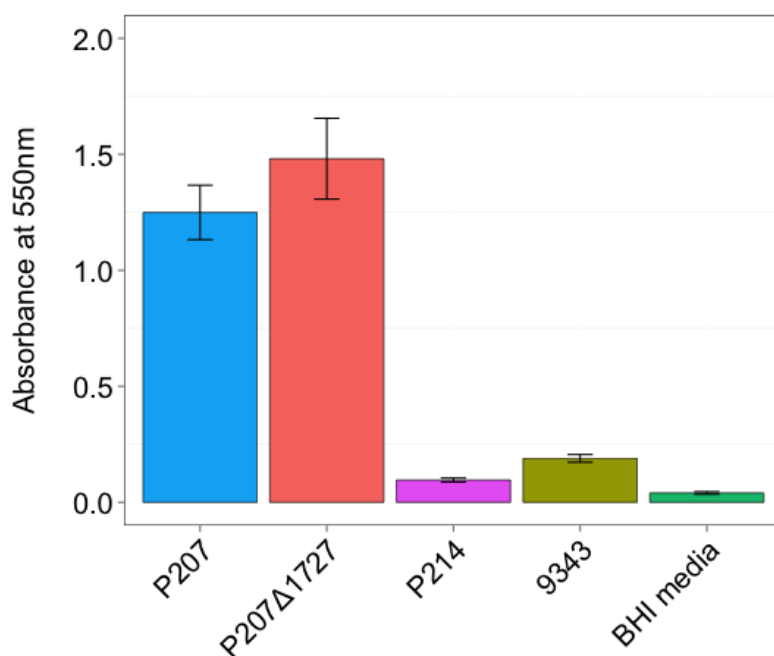


Figure 19: Depiction of the absorbance at 550nm for *B. fragilis* strains, p207, p207 Δ 1727, p214, 9343 and BHI media when stained after o/n anaerobic incubation at 37°C. The higher

the absorbance of the individual strain the more biofilm was formed by the culture strain. The BHI medium served as the background value. The error bars represent the standard deviation by means of the multiple assay set up.

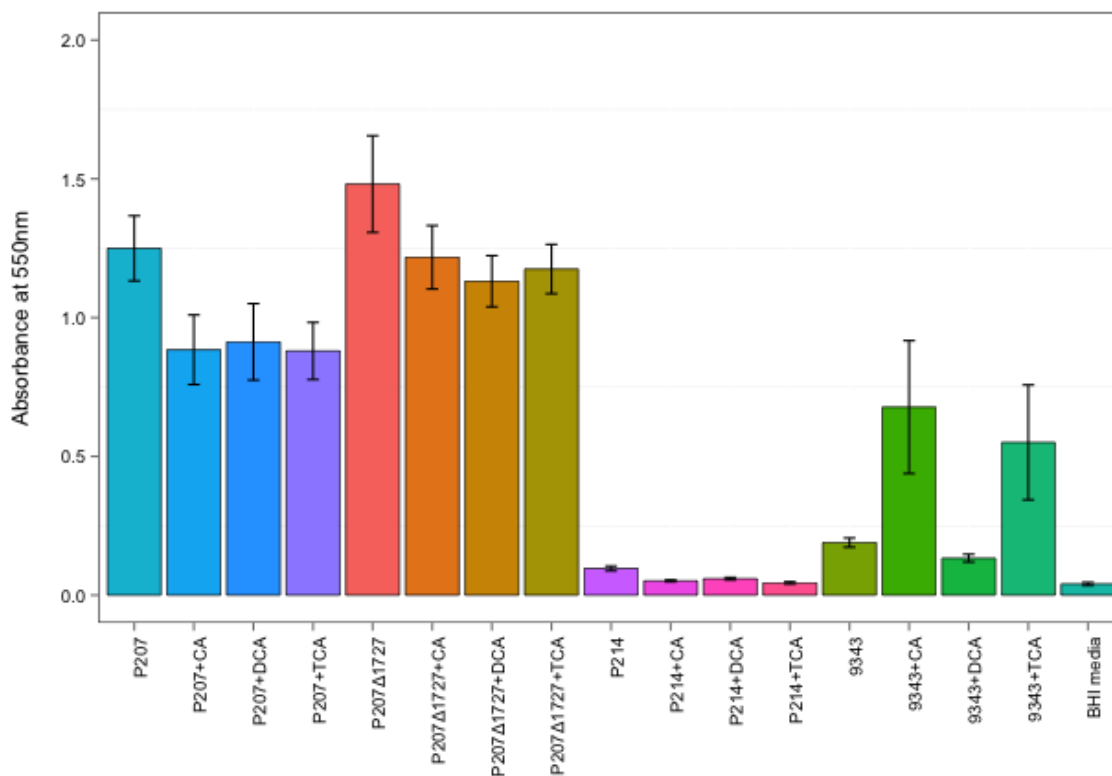


Figure 20: Depiction of the absorbance at 550nm for *B. fragilis* strains, p207, p207Δ1727, p214, 9343 and BHI media when stained after 1h bile acid exposure of mid-log growth cultures. Sodium cholate hydrate (CA), Taurocholic acid sodium salt (TCA) and sodium deoxycholate (DCA). The BHI medium served as the background value. The error bars represent the standard deviation by means of the multiple assay set up.

3.5 Mandeval's capsule stain

B. fragilis p207 and peg.1727_psh mutant were stained by Mandeval's capsule staining method to visualize the capsules of both strains. The acid fuchsin present in the Mandeval's solution interacts with the negative ions of the bacterial cell and stains the cell bright red. Additional acetic acid is contained in the Mandeval's solution and serves to stabilize the structure of the capsule. Congo red solution works as a counterstaining solution and stains the background blue. This staining procedure leads to an unstained, halo capsules between stained cells on a colored background (see figure 21)

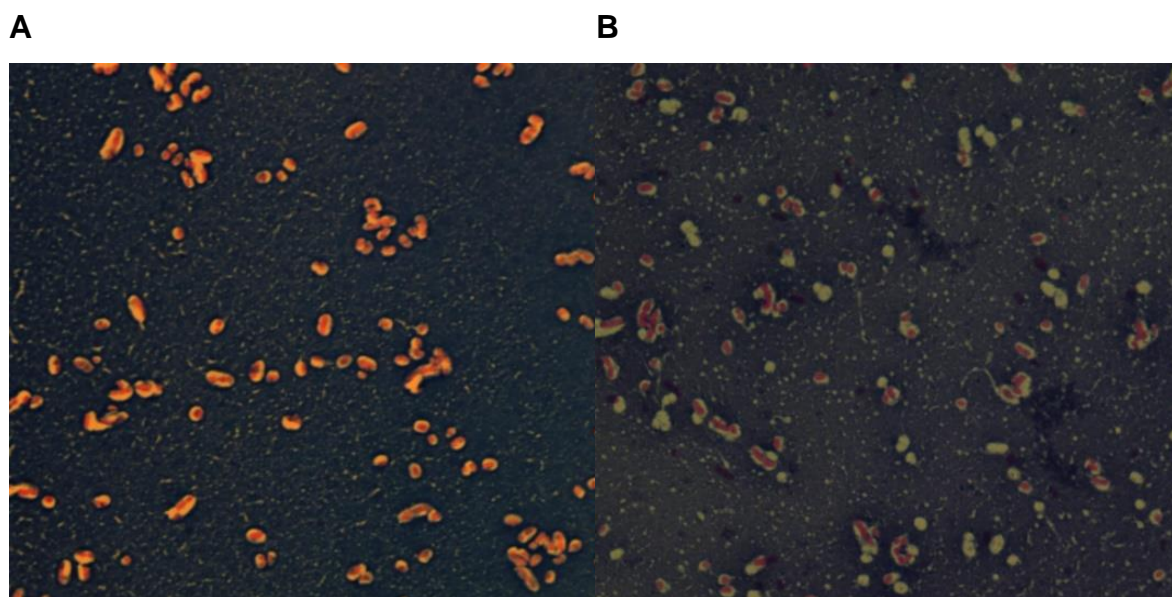


Figure 21: *microscopic image of Mandevilla stained p27 (A) and peg.1727_psh (B) under 1000x magnification*

4 Discussion

In the course of investigating the role of variation in *B.fragilis* capsular polysaccharides in the pathogenesis of pouchitis, the generation of the isogenic mutant lacking the virulence associated gene sequence *peg.1727* on the capsular polysaccharide H, was a successful first step towards understanding the pathogenesis of pouchitis in a greater extent. The deleted sequence is also called antitermination factor UpxY and regulates the downstream biosynthesis of the CpsM protein on the PSH loci, which is suspected to play a role in the capsular transport on the capsular polysaccharides H.

In this study the isogenic capsular polysaccharide H mutant was successfully generated by allelic exchange mutagenesis via a double cross-over event and phenotypic investigations were undertaken.

4.1 Downstream suicide vector mutagenesis confirmation methods

Throughout the suicide vector mutagenesis process certain confirmation PCRs and gel electrophoresis were carried out in order to verify each step as successful. All confirmation PCRs (see Figure 10, 11, 12, 13) were showing the expected bands. In figure 10 the two bands of each 1kb flanking region segment can be clearly seen. This illustrates the successful amplification of the two flanking regions having a length of 1kb.

In the next step these two fragments were fused by together by overlap extension PCR. Through this PCR the *peg. 1727* sequence enclosed by the two flanking regions was deleted. Figure 11 shows the successful fusion since bands at 2000 bp were found, depicting the two fused 1kb segments.

After BamHI digestion and T4 DNA ligation of the fused product *peg.1727* into pKnock in competent *E.coli* S17-1 cells, the product was conjugated into *B.fragilis*. Positive screened colonies with an ampicillin resistance were proven to be successfully conjugated. This can be seen in figure 12 by the bands at 200 bp of each picked

colony. 200 bp depicts the length of the deleted construct in between the two flanking regions. The 200 bp are results of the primers used in the PCR.

These positive screened and confirmed colonies, which have inserted the deletion construct into pKnock in *E.coli* S17-1 cells and which were successfully conjugated into *B.fragilis* were then screened by a counterselectable screening method for potential mutants. This means that the deletion construct, *peg.1727* was integrated into the chromosome of p207 *B.fragilis* and an antibiotic resistance cassette was spilled out simultaneously. Figure 13 ensures the successful generation of the *peg.1727_psh* mutant. The deletion of *peg.1727* in the genome of *B.fragilis* p207 is confirmed by 2 primer sets. The first two primers, DR151 and DR153, enclose the deletion construct and therefore are displaying a shorter sequence of 200 bp for the mutant compared to the 1000 bp sequence of the wild type genomic DNA of p207 (without the deletion). The second set of primers, DR151 and DR152, confirmed the mutagenesis. DR152 is located on the deletion construct itself and therefore cannot amplify in the *peg.1727* mutant. No band is seen in figure 13. In the wild type p207 genomic DNA only a very small fragment of 100 bp is seen. These findings support the successful mutagenesis of p207 *B.fragilis* having knocked out the virulence associated gene sequence *peg.1727* on the capsular polysaccharide H.

Additional a qPCR was performed (see figure 14) confirming the successful deletion of the *peg.1727* sequence. The qPCR shows the expression of the downstream gene sequence, *peg.1740*, in the p207 WT and the *peg.1727_psh* mutant. It clearly depicts the successful deletion of the *peg.1727* sequence since there is no expression in the mutant and a significantly higher expression in the WT. Through the deletion of the *peg.1727* gene sequence also the downstream gene sequence, *peg.1740*, is not expressed anymore confirming the successful mutagenesis.

4.2 Transmission electron microscopy of *peg.1727_psh* and p207

Analyzing the transmission electron microscopy images (see figure 15) a very similar set up made up of the capsule, plasma membrane and cytosol (exterior to interior) can be seen. Since the images depict cross sections of the individual bacterium,

the differences in size evolved. Because of the 3D nature of bacteria the picture could have been taken at different segments. Summed up, the images taken give evidence that between the wild type and the isogenic mutant, there no significant differences in growth morphology.

4.3 Competitive PCR assay between *peg.1727_psh* mutant and P207

Peg.1727_psh mutant and the p207 wild type strain show the same constant growth rate on a logarithmic scale (see figure 16). This leads to the assumption that the knocked out gene sequence on PSH locus has no impact on the growth characteristic of the isogenic mutant, *peg.1727_psh*.

In figure 17 the obtained qPCR data clearly show that the growth of each individual competition culture (competition 1, 2, 3) are nearly identical. The values were obtained by standardization using a standard curve on the basis of the 16S qPCR primers. This gives evidence that the culture conditions throughout the experiment were behaving the same. Therefore the obtained data can be taken into consideration for further evaluations.

Having a look on figure 18, demonstrating the relative abundance of the *peg.1727_psh* isogenic mutant to the wild type strain p207, a certain trend can be seen. While the relative abundance of the WT to the mutant does not change significantly in the time points 0, 2 and 6, there is a 10-fold increase after 4 hours of competition. Since the graph shows a standardized ratio of the wild type p207 over the *peg.1727_psh* mutant a graphic increase corresponds to an increase of the wild type relative to the isogenic mutant and vice versa. At time point 0 the competition was started, meaning that there was no ongoing competition at this point. The genomic number in $t=0$ therefore can be seen as a baseline. After 2 hours of completion the slope slightly declines. This implies a small percentage of out-competition of the *peg.1727_psh* mutant to the p207 WT strain. At time point $t=4$ a 10-fold increase can be seen. This shows that after 4 hours of competition the p207 WT is outcompeting the *peg.1727_psh* mutant. This p207 WT takeover decreases again at time point $t=6$.

Taking these results together it seems that the knock out of the virulence associated gene *peg.1727* on the PSH capsular polysaccharide leads to a relative abundance of the WT to the isogenic mutant. The genetic modifications might have an effect on its fitness and its growth characteristics compared to the p207 WT. The isogenic mutant might lack certain characteristics which make it less compatible regarding the growth and nutrient usage. Nevertheless the assay could be improved by extending the length of the experiment overnight in order to see the competitive behavior between the two strains also in a long term. Additional more runs have to be made to confirm these observations.

4.4 Biofilm formation assay

A biofilm structure is made up of microbial cells and extracellular polymeric substance (EPS) and arise when microbial cells attach to surfaces. It has been investigated that cells associated with a biofilm have specific up- and down- regulated genes and reduced growth rates (Donlan, 2002).

Figure 19 and 20 illustrate the mean absorbance at 550 nm of each individual assay being direct proportional to its biofilm formation. In figure 19 the extent of biofilm formation comparing the four strains p207, p207_peg.1727, p214, 9343 and BHI media only are shown. The human isolate p207 and its own isogenic psh mutant p207_peg.1727 showed a higher biofilm formation compared to p214 and the reference strain 9343. Since there is no significant difference in between of the wild type p207 and its mutant p207_peg.1727, it can be assumed that the deletion of the polysaccharide H gene locus has no influence on the biofilm formation of the mutant. However it can be concluded that the human isolate p207 is prone to develop more biofilm compared to the other human isolate p214.

Having a closer look on figure 20 the biofilm formation responses of the *B. fragilis* strains p207, p207_peg.1727, p214, 9343 and BHI media only to certain bile acid exposure is depicted. The overall picture of p207 and its mutant, forming more biofilm already seen in figure 19, is shown to a similar extent when exposed to bile acids. A general trend in decreasing biofilm formation after CA, DCA and TCA exposure can be observed for the strains p207, p207_peg.1727 and p214. This gives

evidence about the weakening character of bile acids to their biofilm formation. On the other hand 9343 experiences a high biofilm formation increase after CA and TCA exposure and therefore a biofilm promoting character. This observation was already seen and investigated by the group of Pumbwe (Pumbwe et al., 2007). The reason why in DCA exposed 9343 bacteria nearly no biofilm was formed might due to the too high concentration of DCA. This might have led to a fast death of the bacteria and their inability to bind the dye.

All in all these data suggest that in general p207 and its isogenic mutant p207_peg.1727 are forming a greater extent of biofilm, whereas the peg.1727 gene deletion does not have an influence on its formation. Furthermore bile acids do not promote biofilm formation in *B.fragilis* strains except in 9343.

4.5 Mandeval's capsule stain

Bacterial capsules are dense layers made up of high-molecular-weight polysaccharides and optional polypeptides. This viscous layer are secreted by cells and can adhere also to surface of a neighboring cell. Therefore capsules are correlated with biofilm formation and virulence regarding adherence and protection against phagocytosis (Merritt, Kadouri, & Toole, 2005). The bacterial capsule of *B.fragilis* is a major virulence factor and has been investigated to play a major role in inducing abscess formation (Kasper & Seiler, 1975).

Comparing the two microscopic images of both strains, p207 and peg.1727_psh, which were treated by the Mandeval's capsule staining method to visualize the capsules of both strains, no notable differences can be seen (see figure 21). Both show the similar distribution and percentage of unstained halo capsuled and Mandeval stained red cells. The slightly differences in color result from the applied illumination strength.

These findings demonstrate that the knock out of the peg.1727 gene sequence on the PSH locus does not have an effect on its capsule formation. The WT and the mutant show the same capsule morphology.

5 Conclusion and future directions

The results shown and discussed above depict a small step forward in the investigation of the role of *Bacteroides fragilis* capsular polysaccharides variation in the pathogenesis of pouchitis.

Through different confirmatory PCRs and qPCR the successful steps in the progress of generating the isogenic mutant peg.1727_psh was ensured. Having generated this isogenic mutant certain downstream experiments were conducted to investigate possible effects of how the deleted gene sequence peg.1727 influences the virulent characteristic of *B. fragilis*. Using capsular staining, biofilm formation assays and a competitive PCR assay the initial phenotype was characterized. The results show no clear phenotypic and growth differences between the isogenic mutant and the WT. The competitive qPCR assay proposes a small relative abundance of the WT to the isogenic mutant concerning their nutritional competition and fitness.

Future approaches to characterize and the isogenic mutant, peg1727, in a greater extend would include further phenotypic experiments and immunological analyses of the expression of certain pro-and anti-inflammatory cytokines like IL17A, TNF-alpha, IFN-gamma, and IL-10 compared to the p207 wild type.

The successful mutagenesis of the the *B.frag* p207 wild type, knocking out the virulence associated gene peg.1727 on the PSH locus confirms the possibility of applying this method also for future suicide vector mutagenesis using the double-cross-over recombination approach. Future investigations include the generation of an isogenic mutant lacking two virulence associated gene sequences, WcbM and NeuB, on the PSA locus and performing similar phenotypic and immunological characterizations.

All in all a small step in the investigation of the possible role of *Bacteroides fragilis* capsular polysaccharides variation in the pathogenesis of pouchitis has been taken but a successful future is seen possible.

List of References

- Angriman, I. (2014). Relationship between pouch microbiota and pouchitis following restorative proctocolectomy for ulcerative colitis. *World Journal of Gastroenterology*, *20*(29), 9665. <http://doi.org/10.3748/wjg.v20.i29.9665>
- Baumgart, D. C., & Sandborn, W. J. (2012). Crohn's disease. *Lancet*, *380*(9853), 1590–605. [http://doi.org/10.1016/S0140-6736\(12\)60026-9](http://doi.org/10.1016/S0140-6736(12)60026-9)
- Bonizzi, G., Bebien, M., Otero, D. C., Johnson-Vroom, K. E., Cao, Y., Vu, D., ... Karin, M. (2004). Activation of IKKalpha target genes depends on recognition of specific kappaB binding sites by RelB:p52 dimers. *The EMBO Journal*, *23*(21), 4202–4210. <http://doi.org/10.1038/sj.emboj.7600391>
- Cadwell, K., Patel, K. K., Maloney, N. S., Liu, T. C., Ng, A. C., Storer, C. E., ... Virgin, H. W. (2010). Virus-plus-susceptibility gene interaction determines Crohn's disease gene Atg16L1 phenotypes in intestine. *Cell*, *141*(7), 1135–1145. <http://doi.org/10.1016/j.cell.2010.05.009>
- Chatzidaki-Livanis, M., Coyne, M. J., & Comstock, L. E. (2009). A family of transcriptional antitermination factors necessary for synthesis of the capsular polysaccharides of *Bacteroides fragilis*. *Journal of Bacteriology*, *191*(23), 7288–7295. <http://doi.org/10.1128/JB.00500-09>
- Chatzidaki-Livanis, M., Weinacht, K. G., & Comstock, L. E. (2010). Trans locus inhibitors limit concomitant polysaccharide synthesis in the human gut symbiont *Bacteroides fragilis*. *Proceedings of the National Academy of Sciences of the United States of America*, *107*(26), 11976–11980. <http://doi.org/10.1073/pnas.1005039107>
- Coyne, M. J., Weinacht, K. G., Krinos, C. M., & Comstock, L. E. (2003). Mpi recombinase globally modulates the surface architecture of a human commensal bacterium. *Proceedings of the National Academy of Sciences of the United States of America*, *100*(18), 10446–10451. <http://doi.org/10.1073/pnas.1832655100>
- Dalal, S. R., & Chang, E. B. (2014). The microbial basis of inflammatory bowel

- diseases. *The Journal of Clinical Investigation*, 124(10), 4190–6. <http://doi.org/10.1172/JCI72330>
- Domingues, R. M., Cavalcanti, S. M., Andrade, A. F., & Ferreira, M. C. (1992). Sialic acid as receptor of *Bacteroides fragilis* lectin-like adhesin. *Zentralblatt Fur Bakteriologie : International Journal of Medical Microbiology*, 277(3), 340–344. [http://doi.org/10.1016/S0934-8840\(11\)80912-6](http://doi.org/10.1016/S0934-8840(11)80912-6)
- Donlan, R. M. (2002). Biofilms: Microbial life on surfaces. *Emerging Infectious Diseases*. <http://doi.org/10.3201/eid0809.020063>
- García Rodríguez, L. A., Ruigómez, A., & Panés, J. (2006). Acute gastroenteritis is followed by an increased risk of inflammatory bowel disease. *Gastroenterology*, 130(6), 1588–94. <http://doi.org/10.1053/j.gastro.2006.02.004>
- Goldberg, P. A., Herbst, F., Beckett, C. G., Martelli, B., Kontakou, M., Talbot, I. C., ... Nicholls, R. J. (1996). Leucocyte typing, cytokine expression, and epithelial turnover in the ileal pouch in patients with ulcerative colitis and familial adenomatous polyposis. *Gut*, 38(4), 549–53. <http://doi.org/10.1136/gut.38.4.549>
- Half, E., Bercovich, D., & Rozen, P. (2009). Familial adenomatous polyposis. *Orphanet Journal of Rare Diseases*, 4(1), 22. <http://doi.org/10.1186/1750-1172-4-22>
- Huang, J. Y., Lee, S. M., & Mazmanian, S. K. (2011). The human commensal *Bacteroides fragilis* binds intestinal mucin. *Anaerobe*, 17(4), 137–141. <http://doi.org/10.1016/j.anaerobe.2011.05.017>
- K., C., K., D., S., T., P., de A., M., B., M., A., ... A., K. (2011). The genetics of familial adenomatous polyposis (FAP) and MutYH-associated polyposis (MAP). *Acta Gastro-Enterologica Belgica*. Retrieved from <http://ovidsp.ovid.com/ovidweb.cgi?T=JS&PAGE=reference&D=emed10&NEWS=N&AN=2011556471>
- Kasper, D. L., & Seiler, M. W. (1975). Immunochemical characterization of the outer membrane complex of *Bacteroides fragilis* subspecies *fragilis*. *The Journal of*

- Infectious Diseases*, 132(4), 440–450.
- Kircher, A. P., Koruda, Mark J., M. D., & Behrns, Kevin E., M. D. (2003). Ileal Pouch Anal Anastomosis. Retrieved October 28, 2015, from <https://www.med.unc.edu/gi/specialties/ibd/images/treatment-of-ulcerative-colitis/IPAA.pdf>
- Krinos, C. M., Coyne, M. J., Weinacht, K. G., Tzianabos, A. O., Kasper, D. L., & Comstock, L. E. (2001). Extensive surface diversity of a commensal microorganism by multiple DNA inversions. *Nature*, 414(6863), 555–558. <http://doi.org/10.1038/35107092>
- Liu, C. H., Lee, S. M., Vanlare, J. M., Kasper, D. L., & Mazmanian, S. K. (2008). Regulation of surface architecture by symbiotic bacteria mediates host colonization. *Proceedings of the National Academy of Sciences of the United States of America*, 105(10), 3951–3956. <http://doi.org/10.1073/pnas.0709266105>
- Lozupone, C. a., Stombaugh, J. I., Gordon, J. I., Jansson, J. K., & Knight, R. (2012). Diversity, stability and resilience of the human gut microbiota. *Nature*, 489(7415), 220–230. <http://doi.org/10.1038/nature11550>
- Martin, S. T., & Vogel, J. D. (2013). Restorative procedures in colonic crohn disease. *Clinics in Colon and Rectal Surgery*, 26(2), 100–5. <http://doi.org/10.1055/s-0033-1348048>
- McGuire, B. B., Brannigan, a E., & O'Connell, P. R. (2007). Ileal pouch-anal anastomosis. *The British Journal of Surgery*, 94(7), 812–23. <http://doi.org/10.1002/bjs.5866>
- McLaughlin, S. D., Walker, A. W., Churcher, C., Clark, S. K., Tekkis, P. P., Johnson, M. W., ... Petrovska, L. (2010). The bacteriology of pouchitis: a molecular phylogenetic analysis using 16S rRNA gene cloning and sequencing. *Annals of Surgery*, 252(1), 90–98. <http://doi.org/10.1097/SLA.0b013e3181e3dc8b>
- Merritt, J. H., Kadouri, D. E., & Toole, G. A. O. (2005). *Current Protocols in Microbiology*. *Current Protocols in Microbiology*.

- <http://doi.org/10.1002/9780471729259.mc01b01s22>
- Ordás, I., Eckmann, L., Talamini, M., Baumgart, D. C., & Sandborn, W. J. (2012). Ulcerative colitis. *Lancet*, *380*(9853), 1606–19. [http://doi.org/10.1016/S0140-6736\(12\)60150-0](http://doi.org/10.1016/S0140-6736(12)60150-0)
- Ortiz-Martín, I., Macho, A. P., Lambersten, L., Ramos, C., & Beuzón, C. R. (2006). Suicide vectors for antibiotic marker exchange and rapid generation of multiple knockout mutants by allelic exchange in Gram-negative bacteria. *Journal of Microbiological Methods*, *67*(3), 395–407. <http://doi.org/10.1016/j.mimet.2006.04.011>
- Plawski, A., Banasiewicz, T., Borun, P., Kubaszewski, L., Krokowicz, P., Skrzypczak-Zielinska, M., & Lubinski, J. (2013). Familial adenomatous polyposis of the colon. *Hereditary Cancer in Clinical Practice*, *11*, 15. <http://doi.org/10.1186/1897-4287-11-15>
- Pumbwe, L., Skilbeck, C. A., Nakano, V., Avila-Campos, M. J., Piazza, R. M. F., & Wexler, H. M. (2007). Bile salts enhance bacterial co-aggregation, bacterial-intestinal epithelial cell adhesion, biofilm formation and antimicrobial resistance of *Bacteroides fragilis*. *Microbial Pathogenesis*, *43*(2), 78–87. <http://doi.org/10.1016/j.micpath.2007.04.002>
- Pumbwe, L., Skilbeck, C. A., & Wexler, H. M. (2006). The *Bacteroides fragilis* cell envelope: Quarterback, linebacker, coach-or all three? *Anaerobe*. <http://doi.org/10.1016/j.anaerobe.2006.09.004>
- Reyrat, J. M., Pelicic, V., Gicquel, B., & Rappuoli, R. (1998). Counterselectable markers: Untapped tools for bacterial genetics and pathogenesis. *Infection and Immunity*, *66*(9), 4011–4017.
- Samadder, N. J., Gornick, M., Everett, J., Greenson, J. K., & Gruber, S. B. (2013). Inflammatory bowel disease and familial adenomatous polyposis. *Journal of Crohn's & Colitis*, *7*(3), e103–7. <http://doi.org/10.1016/j.crohns.2012.06.021>
- Shapiro, M. E., Kasper, D. L., Zaleznik, D. F., Spriggs, S., Onderdonk, A. B., & Finberg, R. W. (1986). Cellular control of abscess formation: role of T cells in

- the regulation of abscesses formed in response to *Bacteroides fragilis*. *Journal of Immunology (Baltimore, Md. : 1950)*, 137(1), 341–346.
- Shen, B., & Lashner, B. a. (2008). Diagnosis and treatment of pouchitis. *Gastroenterology and Hepatology*, 4(5), 355–361. <http://doi.org/http://dx.doi.org/10.1053/bega.2002.0348>
- Surana, N. K., & Kasper, D. L. (2012). The yin yang of bacterial polysaccharides: Lessons learned from *B. fragilis* PSA. *Immunological Reviews*. <http://doi.org/10.1111/j.1600-065X.2011.01075.x>
- Tamboli, C. P., Neut, C., Desreumaux, P., & Colombel, J. F. (2004). Dysbiosis in inflammatory bowel disease. *Gut*, 53(1), 1–4. <http://doi.org/10.1136/gut.2007.134668>
- Tzianabos, A. O., Kasper, D. L., & Onderdonk, A. B. (1995). Structure and function of *Bacteroides fragilis* capsular polysaccharides: relationship to induction and prevention of abscesses. *Clinical Infectious Diseases : An Official Publication of the Infectious Diseases Society of America*, 20 Suppl 2, S132–S140.
- Tzianabos, A. O., Onderdonk, A. B., Rosner, B., Cisneros, R. L., & Kasper, D. L. (1993). Structural features of polysaccharides that induce intra-abdominal abscesses. *Science (New York, N.Y.)*, 262(5132), 416–419. <http://doi.org/10.1126/science.8211161>
- Wexler, H. M. (2007). *Bacteroides*: The good, the bad, and the nitty-gritty. *Clinical Microbiology Reviews*. <http://doi.org/10.1128/CMR.00008-07>
- Yu, E.-D., Shao, Z., & Shen, B. (2007). Pouchitis. *World Journal of Gastroenterology : WJG*, 13(42), 5598–604. Retrieved from <http://www.pubmedcentral.nih.gov/articlerender.fcgi?artid=4172739&tool=pmc-entrez&rendertype=abstract>
- Zella, G. C., Hait, E. J., Glavan, T., Gevers, D., Ward, D. V, Kitts, C. L., & Korzenik, J. R. (2011). Distinct microbiome in pouchitis compared to healthy pouches in ulcerative colitis and familial adenomatous polyposis. *Inflamm Bowel Dis*, 17(5), 1092–1100. <http://doi.org/10.1002/ibd.21460>

Zhou, J., Thompson, D. K., Xu, Y., & Tiedje, J. M. (2004). *Microbial Functional Genomics. Gene Expression*.